

Tumorigenic Responses of Cancer-Associated Stromal Fibroblasts after Ablative Radiotherapy: A Transcriptome-Profiling Study

Inigo Martinez-Zubiaurre¹, Christopher G. Fenton^{1,2}, Hagar Taman^{1,2}, Ingvild Pettersen¹, Turid Hellevik³, Ruth H. Paulssen^{1,2*}

¹Institute of Clinical Medicine, Tromsø, Norway; ²Microarray Resource Centre Tromsø (MRCT), Institute of Clinical Medicine, University of Tromsø, Tromsø, Norway; ³Department of Oncology, University Hospital of North-Norway, Tromsø, Norway.
Email: *ruth.h.paulssen@uit.no

Received November 7th, 2012; revised December 11th, 2012; accepted December 19th, 2012

ABSTRACT

Cancer-associated fibroblasts (CAFs) are key elements in the progression of cancer and thereby represent important targets for cancer therapies. Increased attention has been given to ablative radiotherapy in the clinics. Therefore, in this study we have aimed at identifying the transcriptional responses occurring in primary CAFs exposed to high-dose irradiation. Established primary CAFs obtained from non-small-cell lung cancer (NSCLC) patient material were irradiated with a single dose of 18 Gy and total RNA was isolated 24 hrs after treatment. Radiation-induced transcriptional alterations were investigated by gene expression analysis using genome-wide microarrays. Obtained results were verified by qRT-PCR of relevant genes. Confirmation of gene expression outcomes was achieved by diverse functional and expression assays including DNA damage response, measurements of reactive oxygen species (ROS) by flow cytometry and senescence-associated β -galactosidase. Irradiation resulted in differential expression of 680 genes of which 557 were up- and 127 down-regulated. Of those, 153 genes were differentially expressed with a fold-change greater than 1.0 and an adjusted p-value less than 0.05 across different comparisons (non-irradiated vs. irradiated). Expression patterns revealed profound changes in biological functions and processes involved in DNA repair, apoptosis, p53 pathway, autophagy, senescence, ROS production and immune response. CAFs display pro- and anti-tumorigenic effects after having received a single high-dose radiation. The measured effects will have an impact on the tumor microenvironment in respect to tumor growth and metastasis.

Keywords: Stereotactic Ablative Radiotherapy (SART); Gene Expression; Cancer-Associated Fibroblasts (CAFs)

1. Introduction

Hypofractionated radiotherapy is emerging as a new treatment option for solid neoplasms of different kinds, including but not limited to medically inoperable stage I non-small-cell lung cancers (NSCLC) [1,2]. Advances in radiotherapy (RT)-technology thus now permit accurate delivery of high-dose (or ablative) RT to target early-stage small tumors with acceptable toxicity to the surrounding normal tissue [3]. Clinical outcomes indicate that ablative RT is associated with improved local control and overall survival compared with conventional RT regimens [2,4]. Despite the encouraging clinical outcomes presented in recent years, little attention has been paid to the biological reactions associated to ablative doses of radiation to tumors.

Tumor progression is a multi-step process orchestrated

by many different cell associated to the malign tissue, such as cancer-associated fibroblasts (CAFs), pericytes, lymphocytes, endothelial cells, extracellular matrix and myeloid cells [5-7]. CAFs are frequently found in the reactive stroma of cancers, and their presence in large number is associated with poor prognosis. When acting on cancer cells, CAFs promote tumor growth and invasion, and enhance angiogenesis by secreting factors that activate endothelial cells and pericytes. Through the secretion of cytokines, CAFs and immune cells can exert both, tumor-suppressing and tumor-promoting effects [8].

Exposure of normal fibroblasts to ionizing radiation has been a common model to study cellular responses to genotoxic stress [9,10]. Aiming for a better understanding of the collateral effects induced by ionizing radiation on normal tissue, some studies have tried to decode the overall changes in gene expression on normal fibroblasts by applying microarray gene technology [9-13]. After

*Corresponding author.

functional categorization of differentially expressed genes, some common traits on altered pathways can be denoted from those studies including DNA damage responses, regulation of cell cycle and proliferation, programmed cell death, p53 target genes, signaling pathways, ROS scavenging and ECM remodeling. Despite the available knowledge on normal tissue fibroblast responses to RT, few reports have focused on the effects of RT on intratumoral reactive stromal fibroblast (CAFs). In a recent study from our laboratory we show that CAF survive to relative high single radiation doses, however the cellular phenotype becomes profoundly altered, characterized by the induction of permanent DNA damage responses and the acquisition of a senescent phenotype and growth arrest [14]. Of note, in that study we show that the expression of some matrix metalloproteinases becomes altered along with overexpression of cell surface integrins.

This work is intended to complement our initial study on radiation-induced responses by tumor-associated fibroblast. Following the rationale of using single high radiation doses to reproduce the effects provoked by stereotactic ablative radiation therapy regimens, in this study we perform transcriptional profiling to rule out in which degree CAFs become pro-tumorigenic and/or anti-tumorigenic after irradiation. To our knowledge this is the first time that such a study has been conducted with freshly prepared CAFs.

2. Materials and Methods

2.1. Human Material, Cell Isolation and CAFs Cultures

Human CAFs were harvested from freshly resected non-small lung cell carcinoma (NSCLC) tumor tissues. Tumors from eight patients with an average age of 58 years (range 44 - 71) were included in this study. The Regional Ethical Committee (REK-Nord) approved the study, and all patients provided written informed consent. Fibroblasts from tumors were isolated and characterized following standard procedures. Briefly, tumor resections were collected and cut into 1 - 1.5 mm³ pieces. Enzymatic digestion of tissues was carried out for 1.5 hrs in 10 mL DMEM/HAM'S F-12 containing bacterial collagenase (Cat.#C-9407, Sigma-Aldrich, St. Louis, MO, USA) at a final concentration of 0.8 mg/mL. Digested tissue was spun down to eliminate collagenase, and resuspended in fresh growth medium (DMEM/HAM'S F-12 supplemented with 10% FBS). Pure fibroblast cultures were obtained by selective cell detachment from the primary culture mix used 2 mM PBS-EDTA solution, and by further cell propagation in the presence of 10% FBS. Cells were used for experiments after the second

passage (2 - 3 weeks). The resulting cultures were characterized for purity and cell identity by flow cytometry using a FITC-conjugated anti-human α -SMA (smooth muscle α -actin) antibody (Abcam; Cat.#ab8211) (data not shown), and by immuno-fluorescent staining with anti-FAP (fibroblast activation protein) antibody (Abcam; Cat.#ab53066) on formalin-fixed CAF cultures.

2.2. Irradiation of Cells

Radiation protocols were established after initial dose-escalating pilot trials. Hence, adherent CAFs cultured in flasks were irradiated at RT with high energy photons produced by a Varian clinical linear-accelerator, delivered as single doses of 2, 6, 12 and 18 Gy. Standard parameters for dose delivery was depth 30 mm, beam quality 15 MV, dose-rate 6 Gy/min and field size 20 × 20 cm. Radiation-doses were confirmed to be correct within an acceptable \pm 4% by Thermo-Luminescent Dosimeters (TLDs) [15]. Cell survival/death after radiation was assessed by light microscopy during the initial three weeks, by automated cell index analyses (xCelligence, Roche) and by MTT cell proliferation and viability assays [16] at different time points [14]. The extent of radiation-induced apoptosis and necrosis in CAFs was determined by staining for annexin V and propidium iodide respectively (data not shown).

2.3. DNA Damage Response (DDR) Foci Staining

CAFs were cultured in 2-well chamber slides (Nunc, Thermo Fisher Scientific, NY, USA), fixed with 4% PFA in PBS for 10 min at RT and permeabilized with 0.2% Triton in PBS for 8 min. Slides were then exposed to blocking buffer containing 2% HSA in PBS, for 30 min at RT. Primary antibody (Rabbit anti human 53BP1; Cat. #ab36823, Abcam, Cambridge, UK) was diluted in blocking buffer and incubated with CAFs for 45 min at RT. After washing with PBS, cells were incubated with secondary antibody (anti rabbit-Alexa546, Cat.#A11010, Molecular Probes/Invitrogen, Leiden, The Netherlands) in blocking buffer, 30 min at RT. A second wash was followed by preparation of slides in DAPI-Fluoromount-G (Cat.#0100-20, Southern Biotech, Birmingham, AL, USA). Specimens were examined in a fluorescence microscope (Zeiss Axiophot, Germany) equipped with a Nikon DS-5MC digital camera, and images were processed with Adobe® Photoshop Software (CS5).

2.4. Senescence Associated β -Galactosidase Assays

CAFs were seeded at a density of 20,000 cells per well in

uncoated 6-well plates and left for attachment for 24 hrs. Adherent cells were irradiated with a single fraction of 18 Gy. Five days post-irradiation, cultures were washed twice in PBS, and fixed for 5 min at RT with freshly prepared paraformaldehyde (2%). β -galactosidase (5-bromo-4chloro-3-indolyl-B-D-galactopyranoside) staining was achieved following instructions from the manufacturer with the "Senescence Cells Histochemical Staining Kit" (Cat.no CS0030, Sigma-Aldrich, St. Louise, MO, USA). The number of β -galactosidase active and senescent cells was determined by counting blue cells under a Nikon Eclipse TS100 model light microscope, and randomly selected fields were photographed at 1000 \times magnification, using an Idea SPOT digital camera.

2.5. ROS Measurements

Intracellular ROS was determined using the CM-H2DCFDA probe (Molecular Probes, Invitrogen, Carlsbad, CA, USA) and flow cytometry. When oxidized, this probe can be detected by fluorescence with excitation at 485 nm and emission at 515 nm. Irradiated CAFs were seeded in 6 well cell culture plates (1×10^5) with 2 ml of complete growth medium and incubated overnight at 37°C, 5% CO₂. The next day, the cells were washed 2 times with Hanks Balanced Salt Solution with CaCl₂ and MgCl₂ (HBSS) (GIBCO, Invitrogen, Carlsbad, CA) and incubated for 30 min with 2.5 μ M CM-H2DCFDA in HBSS. Subsequently the cells were trypsinized, resuspended in 0.5 ml HBSS and immediately analysed by flow cytometry (FACSAria, BD Biosciences). Ten thousand events were collected and analyzed by BD FACSDiva Version 5.0.2. The numbers presented are the median values of the fluorescent intensity.

2.6. RNA Preparation and Quality/Quantity Control

Disruption and homogenization of cells were performed in lysis buffer using the MagNa Lyser Instrument (Roche Applied Science, Germany) and according to the manufacturer's protocol. Subsequently, total RNA was isolated with the MagNa Pure Compact Instrument and the MagNa Pure Compact RNA Isolation Kit (Roche Applied Science, Germany) as previously described [17]. RNA was quantified by measuring absorbance at 260 nm, and RNA purity was determined by the ratios OD260 nm/280 nm and OD230/280 nm using the NanoDrop instrument (NanoDrop[®] ND-1000, Wilmington, USA). The RNA integrity was determined by electrophoresis using the BioRad Experion Bioanalyzer (Data not shown). All the RNA preparations were verified for possible genomic DNA contamination by a minus-RT-PCR conducted directly on RNA samples, with human ge-

nomonic DNA as a positive control and amplification of the human housekeeping gene cyclophilin A. Genomic DNA was not detected in RNA preparations (Data not shown).

2.7. Probe Generation and Array Hybridization

Prior to probe generation 1 μ g total RNA was amplified with the Ambion[®] MessageAmp[™] II aRNA Amplification Kit (Applied Biosystems Inc., USA). RNA samples were transcribed to cDNA using the Invitrogen superscript cDNA synthesis kit (Invitrogen[™], USA). cDNA and Cy3-labelled with the NimbleGen One-Color DNA Labeling Kit and according to the manufacturer's protocol (Roche NimbleGen, Germany). Labelled probes were hybridized to a NimbleGen oligo arrays (12×135 K) with the Roche NimbleGen hybridization system for 16 hours at 42°C. The microarray slides were washed according to the manufacturer's protocol and scanned with an Axon GenePix 4000B scanner (Molecular Devices Inc., USA). Features were extracted by using the NimbleScan v2.5 software.

2.8. Data Analysis and Statistical Analysis

Normalization was carried out using quantile normalization [18]. For the purpose of finding differentially expressed genes, we applied an empirical Bayes analysis using the LIMMA package [19], and significance was determined at the 0.05 level corrected for false discovery rate (FDR) using the Benjamini-Hochberg method [20]. Principal component analysis (PCA) was carried out on the data in order to visualize the data structure and look for potential outlier samples [21]. The differentially expressed genes were annotated by Protein Analysis THrough Evolutionary Relationships (PANTHER; <http://www.panther.org/>). Gene Set Enrichment Analysis (GSEA) was performed using the R statistical package (<http://www.broad.mit.edu/gsea/>). The microarray data were prepared according to minimum information about a microarray experiment (MIAME) recommendations and deposited in the Gene Expression Omnibus (GEO) database: <http://www.ncbi.nlm.nih.gov/geo/>. The GEO accession number for the series is GSE37318.

2.9. Validation of Gene Expression by Quantitative Real-Time Polymerase Chain Reaction

Total RNA was prepared representative for four irradiated and non-treated CAF samples each. These were reverse transcribed using Transcriptor First Strand cDNA synthesis Kit (Roche Applied Science, Germany) as described in the manufacturer's protocol. TaqMan real-time

PCR amplification was performed with an ABI HT7900 Instrument (Applied Biosystems) using primers and probes designed with the Universal Probe Library (Roche Applied Science, Germany) and Taqman[®] Gene Expression Assays (Applied Biosystems). The following primers and probes and inventory assays have been used: MMP11-fw, 5'-GGTGCCCTCTGAGATCGAC-3', MMP11-rev, 5'-TTCACAGGGTCAAACCTTCCAG-3', MMP11 probe #4; ATG16L2-fw, 5'-GGCCACAATGACCAGAAGAT-3', AGT16L2-rev, 5'-GGATGACCTGGGTGCAGT-3', AGT16L2 probe #56; COL7A1-fw, 5'-GCTGGTGCTGCCTTTCTC-3', COL7A1-rev, 5'-TCCAGGCCGAACCTCTGTC-3', COL7A1 probe #71; IL12A-fw, 5'-CACTCCAAAACCTGCTGAG-3', IL12A-rev, 5'-TCTCTTCAGAAGGTGCAAGGGTA-3', IL12A probe #50; GDF15-fw, 5'-CGGATACTCACGCCAGAAGT-3', GDF15-rev, 5'-AGAGATACGCAGGTGCAGGT, GDF15 probe # 28; 5'PPIA-fw, 5'-TGCTGGACCCAACACAAAT-3', PPIA-rev, 5'-CACATGCTTGCCATCCAA-3', PPIA (cyclophilin) probe #48, CYP3A7, Hs00426361_m1; TP53I3, Hs00936520_m1; MDM2, Hs1066930:m1; FDXR, Hs01031618_g1. Samples of each experiment were run in triplicate and averaged for final quantification. The fold-changes were calculated as described previously by analysis of relative gene expression data using real-time quantitative PCR and the $2^{-\Delta\Delta(T)}$ method [22].

3. Results

3.1. Survival Rates and CAFs Responses to Ablative Radiation Doses

All the data generated in this study come from cell cultures directly prepared from lung tumor specimens obtained from 8 different donors after surgical resection (**Figure 1**). In a previous study from our group we describe in detail the isolation and characterization of the tumor fibroblast cultures that have been used also for this study [14].

Of note, flow cytometry analyses using the fibroblast specific marker α -SMA reveal a purity above 99.5%, which gives full credibility to the data generated with this material. The intrinsic radioresistance of CAFs in dose escalating trial experiments have also been evaluated and described by us previously [14]. A single dose of 18 Gy happens to be sub-lethal for CAFs, however we have observed that single doses above 12 Gy induce enduring DNA damage responses (nuclear foci of 53BP1) and the cells enter into a permanent cell growth arrest or senescence. Hence, based on our previous experience we have chosen the use of a single dose of 18 Gy as the basis

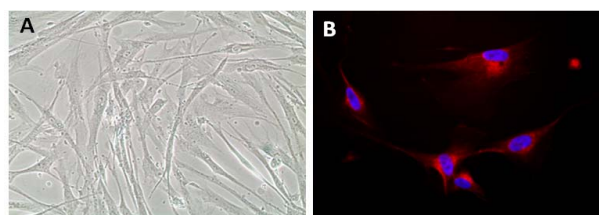


Figure 1. A 200× magnification phase contrast micrograph of three weeks old CAFs in monolayer culture is shown in (A). CAFs are characterized by immunostaining with anti-FAP (fibroblast activating protein), a specific marker of reactive fibroblasts (400× magnification) and as shown in (B).

protocol for conducting this study. In previous studies done by others on normal fibroblasts, 24 hours post-irradiation seems to be the time point where the largest number of genes is altered [10]. We have therefore set up 24 hours as the single and most relevant time point to analyse changes in gene expression.

3.2. Radiation-Induced Gene Expression

Large scale molecular responses in CAFs obtained from NSLC patient material to ablative doses of radiation were studied by measuring genome-wide transcript-level changes using human genome survey microarrays as described in Materials and Methods. After pre-processing and normalization, a total of 680 differentially expressed were found in the group of irradiated CAF samples, of which 127 genes were down- and 553 were up-regulated transcripts with $p < 0.05$ (**Supplemental list 1**). Of all differentially expressed genes, 601 could be annotated by GO terms for biological processes in Kegg (<http://www.genome.jp/kegg/>) and are summarized in **Supplemental list 2**. Principal component analysis (PCA) revealed that the major variability in the data set is caused by the difference between irradiated and non-irradiated CAFs (Data not shown). The number and distribution of 153 differentially expressed genes with fold change greater than 1 and an adjusted p-value less than 0.05 across different comparisons is shown in **Figure 2**.

3.3. Radiation-Induced Pathways after Functional Categorization

Candidate genes which relate to senescence have been extracted from the GenAge database (<http://genomics.senescence.info/genes/human.html>) (**Table 1**). In addition, the expression levels of some differentially expressed genes found in this study have been verified by qRT-PCR (**Table 2**).

Differentially expressed genes were annotated with PANTHER (<http://www.pantherdb.org/>) to different biological processes: cell cycle regulation and DNA repair

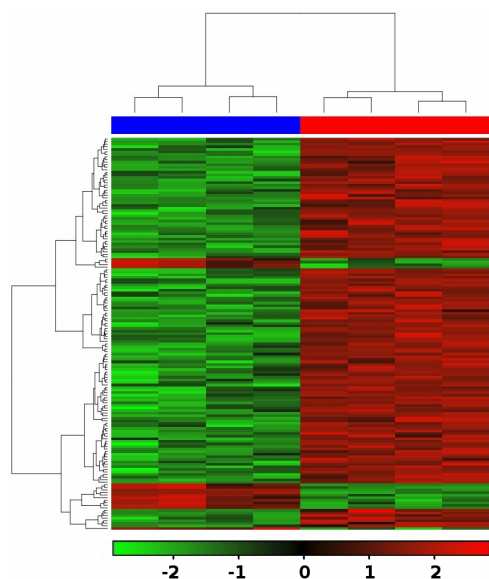


Figure 2. Heatmap of 153 differentially expressed genes in irradiated CAFs with fold change greater than 1.0 and an adjusted p-value less than 0.05 are shown. CAF samples are shown as red bar (top) and non-irradiated CAF samples as blue bar (top). Legend (bottom) shows the fold change [\log_2 (radiated) - \log_2 (normal)] color coded values in the heatmap.

(**Table 3**), oxidative stress (**Table 4**), apoptosis (**Table 5**), autophagy (**Table 6**), and cell communication/cell adhesion (**Table 7**).

Increased expression levels of interleukin 12 (IL-12), autophagy related protein 16-2 (ATG16L2), growth differentiation factor 15 (GDF15), cytochrome P450, family 3, subfamily A, polypeptide 7 (CYP3A7), NADH adenodoxin osireductase (FDXR), transformed 3t3 cell double minute 2 (MDM2), collagen type 7 alpha 1 (COL7A1) and stromelysin 3 (MMP11), and tumor protein p53 inducible protein 3 (TP53IP3) were confirmed by qRT-PCR (**Table 2**). **Figure 3** depicts differential expression of 37 selected genes that are discussed in more detail below.

3.4. Validation of Expression Data by Functional Assays

Gene expression analysis indicated that some p53-dependent pathways and the cell cycle regulation machinery were altered after IR. One end point of such disturbances is the development of stress-induced cellular senescence. In our previous study we have performed quantitative and qualitative measurements of senescence on CAFs after exposure to either high single dose or fractionated

Table 1. Differentially expressed genes related to ageing/senescence in irradiated CAFs.

HGNC Symbol	Common name	Biological process	FC*
APTX	aprataxin	stress response	+1.3
BAX	BCL2-associated X protein	apoptosis	+1.7
BLM	Bloom syndrome, RecQ helicase-like	mitosis	-5.2
HMGB1	high-motility group box 1	stress response	-1.6
HRAS	v-Ha-ras Harvey rat sarcoma Viral oncogene homolog	apoptosis, cell cycle, growth & development	+1.9
HSF1	heat shock transcription factor 1	stress response	+1.5
HSPA8	heat shock 70kDa protein 8	stress response	-1.2
MDM2	Mdm2 p53 binding protein homolog	cell cycle, apoptosis	+3.0
NRG1	neuregulin 1	apoptosis, growth & development	+6.9
PARP1	poly (ADP-ribose) polymerase 1	apoptosis	-1.2
PCNA	proliferating cell nuclear antigen	cell cycle	+3.3
PIN1	peptidylpropyl cis/trans isomerase 1	Apoptosis cell cycle	+1.4
PML	promyelocytic leukemia cell cycle	apoptosis,	+1.4
PPM1D	protein phosphatase 1D cell cycle	stress response,	+1.6
PTPN11	protein tyrosine phosphatase, non-receptor type 11	growth & development	-1.3
RCF4	replication factor C4	unclassified	-1.7
SUMO1	SMT3 supressor of mif two 3 homplog 1	apoptosis	-1.2
STE24	zinc metallopeptidase	unclassified	-1.5

*Values are shown as fold-change representing eight independent microarray experiments.

Table 2. Verification of selected expressed genes in irradiated CAFs by qPCR.

Gene Symbol	Gene name	FC*	qPCR [#]
ATG16L2	autophagy related protein 16-2	+1.89	+1.46 ± 0.296
COL7A1	collagen type 7 alpha 1	+3.04	+10.50 ± 0.333
CYP3A7	cytochrome P450, family 3, subfamily A, polypeptide 7	+3.20	+3.30 ± 0.078
FDXR	NADH adrenodoxin oxidoreductase	+3.90	+5.22 ± 0.319
GDF15	growth differentiation factor 15	+3.80	+2.14 ± 0.008
IL12A	interleukin 12A	+2.23	+2.13 ± 0.001
MMP11	stromelysin-3	+2.42	+1.93 ± 0.310
MDM2	transformed 3t3 cell double minute 2	+2.36	+3.32 ± 0.224
TP53I3	tumor protein p53 inducible protein 3	+2.12	+1.76 ± 0.361

*Values are shown as fold-change (FC) representing eight independent microarray experiments and [#]RT-PCR validations in triplicate ± S.D. of each representative RNA sample.

Table 3. Differentially expressed genes (p < 0.05) related to cell cycle regulation and DNA repair in irradiated CAFs.

HGNC Symbol	Common name	FC*
ANAPC2	anaphase promoting complex subunit 2	+2.0
ANAPC11	anaphase promoting complex subunit 11	+1.5
APTX	aprataxin	+1.3
ASCC3	activating signal cointegrator 1 complex subunit 3	+1.7
BLM	Bloom syndrome protein	-5.2
CEP164	centrosomal protein 164kDa	+1.7
CCNE2	cyclin E2	+4.4
CCNG1	cyclin G1	+1.2
CCNK	cyclin K	+1.2
CCNL2	cyclin L2	+1.5
CDC6	cell division cycle, 6 homolog	-3.2
CDC34	cell division cycle, 34 homolog	+1.4
DDB2	damage-specific DNA binding protein 2	+2.6
DNASE1	deoxyribonuclease 1	+1.4
DTL	denticleless homolog	-5.0
H2BFS	H2B histone family, member S	+1.7
HIST1H2AC	histone cluster 1, H2ac	+1.9
HIST1H2BE	histone cluster 1, H2be	+1.6
HIST1H2BF	histone cluster 1, H2bf	+2.4
HIST1H2BK	histone cluster 1, H2bk	+2.5
HIST1H2BO	histone cluster 1, H2bo	+1.6
LIG1	DNA ligase 1	+2.4
LZTR1	leucine zipper-like transcriptional regulator 1	+1.4
MCM10	minichromosome maintenance complex component 10	-8.3
MKNK1	MAP kinase-interacting serine/threonine-protein kinase 1	+1.4
MNS1	meiosis-specific nuclear structural protein 1	-2.3
MSH2	DNA mismatch repair protein Msh2	-1.5
PCNA	proliferating cell nuclear antigen	+3.3
PFTK1	serine/threonine protein kinase PFTFAIRE-1	-1.5
PIN1	peptidylprolyl cis/trans isomerase, NIMA-interacting 1	+1.4
POLL	DNA polymerase lambda	+1.5
PTPRU	receptor-type tyrosine-protein phosphatase U	+1.8
PRKX	serine/threonine protein kinase	+1.5
RAGE	MAPK/MAK/MRK overlapping kinase	+1.6
RBL2	retinoblastoma-like protein 2	-1.6
RFC4	replication factor C subunit 4	-1.7
RPA4	replication protein A4	+1.8
SMG6	telomerase-binding protein EST1A	+1.4
TRIM28	transcription intermediary factor 1-beta	+1.4
XPC	xeroderma pigmentosum, complementation group	+1.8

*Values are shown as fold-change (FC) representing eight independent microarray experiments.

Table 4. Differentially expressed genes (p < 0.05) related to oxidative stress in irradiated CAFs.

HGNC Symbol	Common name	FC*
ACAD10	acyl-CoA dehydrogenase family member 10	+1.3
ACO2	aconitate hydratase, mitochondrial	+1.5
AMT	aminomethyl transferase, mitochondrial	+1.5
BCS1L	mitochondrial chaperone BCS1	+1.5
CYC1	cytochrome c1, heme protein, mitochondrial	-1.3
CYP3A4	cytochrome P450, family 3, subfamily A, polypeptide 4	+3.2
CYP3A7	cytochrome P450, family 3, subfamily A, polypeptide 7	+3.2
DECR1	peroxisomal 2, 4-dienoyl-CoA reductase	+1.9
FDXR	NADH adrenodoxin oxidoreductase	+4.1
FOXRED1	FAD-dependent oxidoreductase domain-containing protein 1	+1.9
GFER	FAD-linked sulfhydryloxidase ALR	+1.6
GGT1	gamma-glutamyltransferase 1	+2.5
IDH3B	isocitrate dehydrogenase [49] subunitbeta, mitochondrial	+1.4
NDUFA2	NADH dehydrogenase (ubiquinone) 1 alpha subcomplex, 2	+1.6
NDUFA12	NADH dehydrogenase (ubiquinone) 1 alpha subcomplex, 12	+1.2
NDUFA13	NADH dehydrogenase (ubiquinone) 1 alpha subcomplex, 13	+1.5
NDUFC1	NADH dehydrogenase (ubiquinone) 1, subcomplex unknown	+1.8
PTGES2	prostaglandin E synthase 2 truncated form	+1.3
SESN1	sestrin-1	+1.9
SESN3	sestrin 3	-1.6
TP53I3	tumor protein p53 inducible protein 3	+2.1
UCRC	cytochrome b-c1 complex subunit 9	+1.3

*Values are shown as fold-change (FC) representing eight independent microarray experiments.

Table 5. Differentially expressed genes (p < 0.05) related to apoptosis in irradiated CAFs.

HGNC Symbol	Common name	FC*
<i>Anti-apoptotic</i>		
BAG3	BCL2-associated athanogene 3	+4.4
BCL2L1	BCL2-like 1	+2.4
BEX2	brain expressed X-linked 2	+1.9
SYVN1	synovial apoptosis inhibitor 1, synoviolin	+1.5
TRIAP	TP53 regulated inhibitor of apoptosis 1	+1.9
<i>Pro-apoptotic</i>		
CRADD	CASP2 and RIPK1 domain containing adaptor with death domain	+1.6
LRDD	leucine-rich repeats and death domain containing	+4.1
NALP1	death effector filament-forming ced-4-like apoptosis protein	+1.8
PYCARD	caspace recruitment domain-containing protein 5	+1.4
<i>Other apoptotic</i>		
AKT3	v-akt murine thymoma viral oncogene homolog 3	-1.3
ASAH3L	alkaline ceramidase 2	+2.9
BAG5	Bag family molecular chaperone regulator 5	-1.3
BAX	BCL2-associated X protein	+1.7
BLNK	B-cell linker protein	+6.5
CYFIP2	cytoplasmic FMR1-interacting protein 2	+9.0
GSK3A	glycogen synthase kinase 3 alpha	+1.3
MDM2	Mdm2 p53 binding protein homolog	+2.3
SGK2	serine/threonine protein kinase Sgk2	-2.6
TIGAR	TP53-induced glycolysis and apoptosis regulator	+2.2
TP53I3	tumor protein p53 inducible protein 3	+2.1

*Values are shown as fold-change (FC) representing eight independent microarray experiments.

Table 6. Differentially expressed genes (p < 0.05) related to autophagy in irradiated CAFs.

HGNC Symbol	Common name	FC*
AP1B1	adaptor-related protein complex 1, beta 1 subunit	+1.7
AP3B2	adaptor-related protein complex 3, beta 2 subunit	+2.9
ATG4D	ATG4 autophagy related 4, homolog D	+1.4
ATG16L2	ATG16 autophagy related 16-like 2	+1.9
APIG2	adaptor-related protein complex 1, gamma 2 subunit	+1.6
AP1S1	adaptor-related protein complex 1, sigma 1 subunit	+1.7
CLCA2	chloride channel accessory 2	+4.0
CLTB	clathrin	+1.2
HMGB1	high-mobility group box 1	+1.6

*Values are shown as fold-change (FC) representing eight independent microarray experiments.

Table 7. Differentially expressed genes (p < 0.05) related to cell communication/cell adhesion and other biological processes in irradiated CAFs.

HGNC Symbol	Common name	FC*
ADAM9	ADAM metalloproteinase domain 9	-1.5
AGRN	agrin	+1.5
ANGPT1	angiopoietin 1	-1.4
AREG	amphiregulin	+2.7
ARFGAP1	ADP-ribosylation factor GTPase-activating protein 1	+1.4
ARHGAP30	Rho GTPase-activating protein 30	+1.9
BAIAP2	brain-specific angiogenesis inhibitor 1-associated protein 2	+1.3
CLCA2	chloride channel accessory 2	+4.0
COL7A1	collagen, type VII, alpha	+3.0
CSF1	colony-stimulating factor 1	+1.7
DUSP6	dual specificity protein phosphatase 6	+1.5
DYNC1H1	cytoplasmic dynein 1 heavy chain 1	+1.5
EPS8L2	Epidermal growth factor receptor pathway substrate 8-related protein 2	+2.2
GDNF	glial cell line-derived neurotrophic factor	+3.4
GPC1	glypican 1	+1.9
GPC6	glypican 6	-1.5
HYAL3	hyaluronidase 3	+2.5
IL12A	interleukin 12A	+3.1
IL1F10	interleukin 1 family, member 10 (theta)	+1.3
KIF1C	kinesin-like protein 1C	+1.8
KIF7	kinesin-like protein F7	+1.3
MGP	matrix Gla protein	-1.7
MIB2E3	ubiquitin-protein ligase MIB2	+2.0
MMP11	matrix metalloproteinase 11 (stromelysin 3)	+2.4
NINJ1	ninjurin 1	+1.9
NRG1	neuregulin 1	+5.7
PIK4CA	phosphatidylinositol 4 kinase, alpha	+1.5
PLCD1	phospholipase C, delta 1	+1.9
PLEKHH3	plekstrin homology domain-containing family H member 3	+2.0
PLK3	polo-like kinase 3	+2.0
PLXNA4B	plexin A4	-1.9
PLXNB1	plexin B1	+2.1
PLXNB3	plexin B3	+3.4
PPM1D	protein phosphatase 1D	+1.6
PPP2R5C	protein phosphatase 2, regulatory subunit B, gamma	-1.4
PROCR	endothelial protein C receptor	+2.0
RAP2B	ras-related protein rap-2b	+1.8
RBP2	retinol-binding protein 2	+2.0
S100A1	S100 calcium binding protein A1	+1.6
SEPT10	septin 10	-1.3
SETD7	SET domain containing (lysine methyltransferase) 7	-1.2
SFN	stratifin	+2.2
SHC4	SHC-transforming protein 4	+3.6
STXBP2	syntaxin-binding protein 2	+1.8
SYMPK	symplekin	+1.3
THSD1	thrombospondin, type 1, domain containing 1	+2.6
TUPGCP3	gamma-tubulin complex component 3	-1.3
TUPGCP6	gamma-tubulin complex component 6	+1.7
VWCE	von Willebrand factor and EGF domain-containing protein	+8.7

*Values are shown as fold-change (FC) representing eight independent microarray experiments.

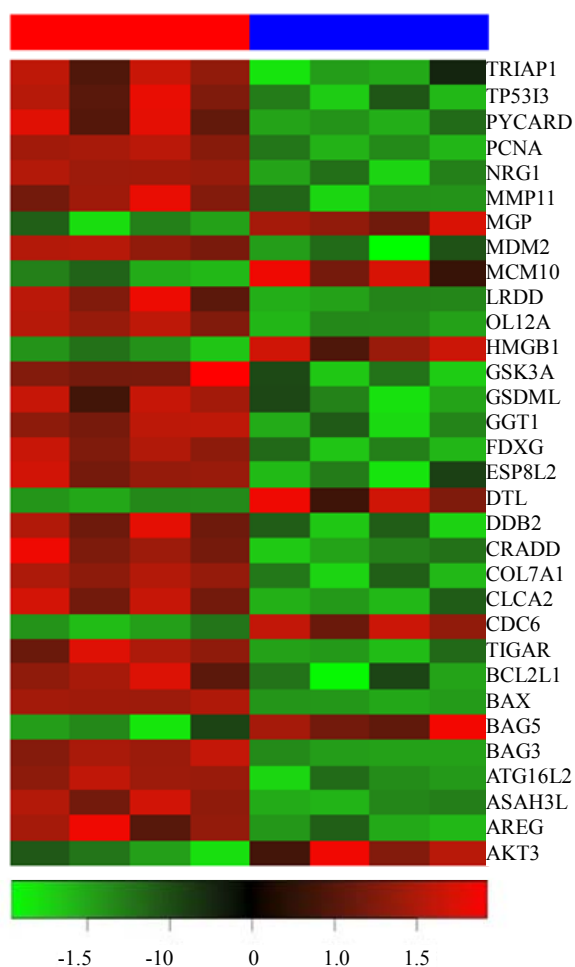


Figure 3. Heatmap of 37 selected genes in irradiated CAF samples are shown as red bar (top) and non-irradiated CAF samples as blue bar (top). Legend (bottom) shows the fold change $[\log_2(\text{radiated}) - \log_2(\text{normal})]$ color coded values in the heatmap.

irradiation [14]. Our data show a potent and permanent induction of cell senescence after a single insult of 18 Gy and **Figure 4** illustrates the acquisition of the senescent phenotype by CAFs after exposure to 18 Gy.

One of the most drastically altered pathways after irradiation corresponded to DNA damage responses and chromatin rearrangements (**Table 3**). Previously we have conducted quantitative dose-dependent measurements of DNA damage and repair induced by IR on CAFs. In that study we show that IR provoke substantial DNA damage even at low radiation doses, however we saw that arising nuclear foci were able to resolve at radiation doses lower than 12 Gy. After a single dose with 18 Gy a strong and permanent DNA damage response on cells was established. An illustration of these observations is presented in **Figure 5**.

Intracellular levels of reactive oxygen species (ROS)

were determined as described in detail in the Materials & Methods. ROS production by CAFs was significantly increased in irradiated CAFs (**Figure 6**). Elevated ROS production has been found to be predominantly a consequence of altered mitochondrial gene expression (**Table 4**). Increased expression of cytochrome P450, family 3, subfamily A, polypeptide 7 (CYP3A4) and NADH adrenodoxin oxidoreductase (FDXR) was confirmed by qPCR (**Table 2**).

Genes associated with regulation of autophagy and apoptosis were also transformed after IR (**Table 5** and **Table 6**). However, expression of apoptotic genes like MDM2 p53 binding protein homolog (MDM2) and tumor protein p53 inducible protein 3 (TP53I3), and expression of ATG16 autophagy related 16-like 2 (ATG16L2) gene was confirmed by qPCR (**Table 2**).

In pilot experiments, apoptosis and autophagy were measured on CAFs at different points after IR by staining for annexin V on living cells and by using Cyto-ID Autophagy Detection Kit (ENZO life Sciences) respectively (data not shown). These assays failed to show induction of neither apoptosis nor autophagy in CAFs for up to two weeks after exposure to 18 Gy, indicating that the counter balance between the pro- and anti-signaling mechanisms prevented the ultimate induction of such pathways.

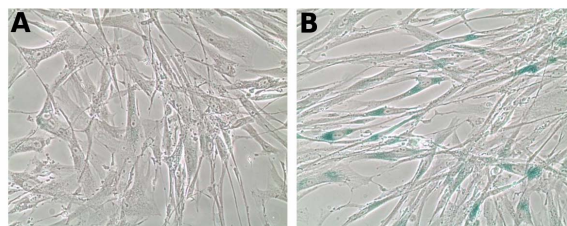


Figure 4. Induction of cellular senescence was determined by β -galactosidase staining assay. Adherent CAFs were irradiated (1×18 Gy) and 5 days later examined for the expression of intra-cytoplasmic β -galactosidase. (A) control conditions (0 Gy); (B) irradiated cultures (18 Gy).

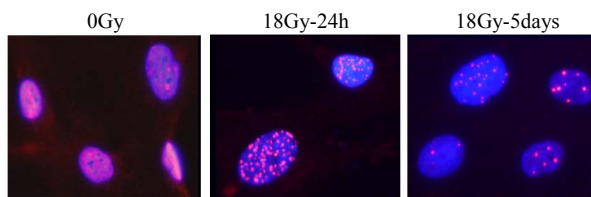


Figure 5. Persistent DDR (DNA Damage Response). Cells were immunostained for 53BP1 (red, Alexa546) and nuclei were stained with DAPI (Blue). Homogenous nuclear staining of 53BP1 was observed in non-irradiated cells, whereas numerous nuclear foci were observed 24 hours post-irradiation. After five days most cells still demonstrated multiple nuclear foci, with a reduced number of foci when compared to earlier time points.

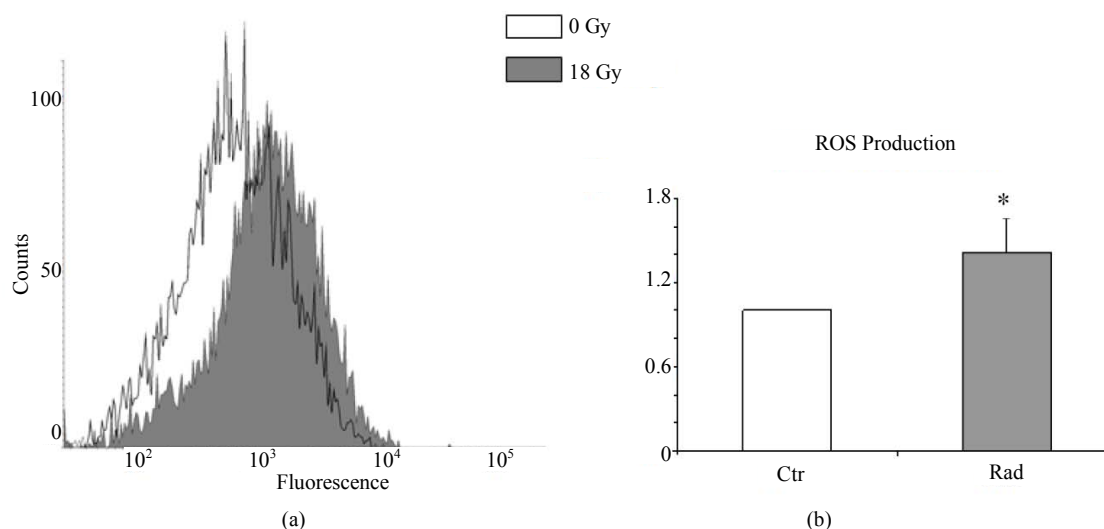


Figure 6. The intracellular ROS production was counted as total H_2O_2 accumulated in cells 24 hours after IR. H_2O_2 levels were determined in CAFs from 4 different donors by incubating cells with 2.5 mM CM-H2DCFDA for 30 minutes followed by flow cytometric analyses. Ten thousand events were collected for each measurement and the mean values of the relative fluorescence were registered. Panels in (a) illustrate ROS staining in CAFs from one representative donor. Continuous lines correspond to fluorescence patterns in non-irradiated cells; filled peaks correspond to fluorescence intensity in irradiated cells. In (b), mean fluorescent intensities resulting from FACS analysis from four randomly selected donors is presented. Fluorescence intensity from non-irradiated cultures was averaged and normalized (open bars) whereas the irradiated counterparts are presented with X-fold increase in surface labeling relative to control cells (filled bars). The asterisk (*) indicates significant differences ($p < 0.05$) in mean values when compared to the levels in untreated cells.

In addition, the increased expression of genes involved in cell adhesion, collagen type VII alpha (COL7A1) and stromelysin 3 (MMP11), and the cytokine interleukin 12A (IL2A) has been confirmed accordingly (Table 2).

4. Discussion

The aim of this study was to examine the impact of high-dose ionizing radiation on activated cancer-associated fibroblasts (CAFs) and to predict the consequences of the induced changes on post-radiation tumorigenesis. The overall study showed that approximately 80 % of all differentially expressed genes were up-regulated and 20 % were down-regulated after treatment (Supplemental list 1). In line with previous reports performed on normal tissue fibroblasts, our data show that a large extent of differentially expressed genes belongs to cellular mechanisms related to cell stress, cell cycle, apoptosis, DNA repair, and other pro-survival pathways. It is expected that ionizing radiation induces severe genotoxic stresses in cells, followed by alterations on the expression of genes involved in biological processes like DNA repair, cell proliferation, cell cycle, apoptosis and p53 pathway as has been also shown in a previous study with primary human skin fibroblasts [9]. Cell proliferation and cell cycle checkpoints are some of the pathways profoundly affected by ablative doses of ionizing radiation (AIR) on CAFs. Hence, a list of genes involved in cell cycle regu-

lation such as cell division cycle homologs CDC6 and CDC34, proliferating cell nuclear antigen (PCNA) and different cyclins are all up-regulated, whereas denticless protein homolog (DTL) and minichromosome maintenance component 10 (MCM10) are down-regulated (Table 3). Secondly, (RPA2), Mdm2 p53 binding protein homolog (MDM2), and damage-specific DNA binding protein 2 (DDB2), were both up-regulated. In line with our observations, an increased expression of cyclins and PCNA has been also observed in normal fibroblasts after lower dose ionizing radiation [11]. In addition, many histones showed increased expression (Table 3). They do not only play an important role in transcription regulation, but are also important team players in DNA repair mechanisms by being responsible for sustaining chromosomal stability [23]. Putting it together, these data suggest that CAFs intend to counteract mitotic catastrophe after irradiation.

In normal fibroblast radiation exposure, as well as administration of genotoxic agents, are able to induce growth arrest, a phenomenon described as cellular senescence [24]. Senescence is often accompanied by stimuli like oxidative DNA damage, and a compromised replicative cell cycle [25]. Although cellular senescence can be ascribed as a self-regulated tumor suppressor mechanism, thereby protecting the organisms from developing cancer, it has been acknowledged that senescent

stromal fibroblasts are able to expedite epithelial tumorigenesis [26]. Ionizing radiation of CAFs revealed differential expression of a considerable number of genes that are related to senescence and ageing. Candidate genes listed have been shown to be involved in senescence at different extents (**Table 1**).

In our hands, high-dose ionizing radiation results in an increase of reactive oxygen species (ROS) formation in CAFs. The provoked enhanced ROS production is reflected by alterations in mainly mitochondrial-generated ROS rather than activation of the NADPH-oxidase (NOX) system (**Figure 3** and **Table 4**). Of note, the disturbances in the redox homeostasis of irradiated CAFs have the potential to lead to increased tumor growth [27]. Previous studies have shown that normal fibroblasts express multiple ROS scavenger genes when irradiated with lower doses [13]. Here, enhanced expression was only observed for one ROS scavenger, namely gamma glutamyl transferase 1 (GGT1).

The expression of genes involved in the regulation of apoptosis was also modified after AIR, including both pro- and anti-apoptotic signaling pathways (**Table 5**). Thus, the transcription of genes involved in caspase-mediated apoptosis (caspase recruitment domain-containing protein (PYCARD) and caspase and RIP adapter with death domain (CRADD) was enhanced, which correlates with observations made in irradiated normal tissue fibroblast [11]. However, in our *in vitro* assays we could not observe apoptotic cells during the first two weeks post irradiation. Taken these observations together, we may conclude that the anti-apoptotic signals had stronger influence on the final outcomes on cells.

Of importance, a number of genes regulated by or connected to the tumor suppressor gene p53 were shown to be up- or down regulated. The observed over-expression of MDM2 can result in excessive inactivation of tumor protein p53 in CAFs, thereby diminishing its tumor suppressor function and therefore affecting tumorigenesis [28] or may act in a p53-independent manner as an oncogene [29]. It is hereby noted that nine different MDM2 transcripts showed increased expression levels (see also **Supplemental list 1**). Their functional and not yet defined biological implications on the tumor micro-environment still needs to be elucidated [30]. Increased expression levels for MDM2 variants have been reported to be related to radio-sensitivity in the lung [31], and implies the possibility that CAF to some extent become radio-resistant after treatment [32]. On the other hand, up-regulation of the TP53-induced glycolysis and apoptosis regulator (TIGAR) may protect irradiated CAFs against reactive oxygen species and apoptosis induced by TP53/p53. It has been shown that fibroblasts are also able to induce an up-regulation of TIGAR expression in

cancer cells, thereby protecting cancer cells against apoptosis and autophagy, as recently described in an autophagic tumor stroma model of cancer [33].

Autophagy, which can be ascribed as both cell survival and cell death mechanism has been shown to be activated in tumor cells after ionizing radiation [34]. Here, enhanced expression of a large number of other genes related to autophagy has been observed (**Table 6**). A role for autophagy in CAFs has been recently shown to be linked to promotion of tumor cell survival [33]. However, the establishment of an autophagic response in CAFs after AIR still needs to be confirmed, and whether such stress-induced changes occurring in CAFs could have an impact on tumor cells also remains to be determined.

Pro-angiogenic signals released by CAFs contribute importantly to the overall sustainability of tumors [35,36]. However, the observed decreased expression of the pro-angiogenic factor angiopoietin 1 ANGPT1, a factor that mediates reciprocal interactions between the endothelium and surrounding matrix [37], might result in suppressed tumor growth. Several anti-angiogenic molecules showed increased expression in CAFs after high-dose ionizing radiation which might have a direct impact on tumor growth. The matrix-derived angiogenesis inhibitor thrombospondin type I, domain containing 1 (THSD 1) [38], which is able to confer signals like thrombospondin 1 [39-41], and interleukin 12A (IL-12A) [42], both may be able to reduce tumor growth rate. In contrast, several semaphorin receptors which are able to confer both, pro- and anti-angiogenic signals are differentially expressed in irradiated CAFs (**Table 7**). The observed differential expression of plexins PLXNB1, PLXNB3 and PLXA4B imply a role for CAFs on endothelial cell migration [43]. Their role in normal lung and in invasive growth and cell migration in lung cancer has been discussed [44,46]. Interestingly, the activation of PLXNB1 and PLXNB3 in irradiated CAFs might inhibit integrin-based adhesion and cell migration on the ECM as has been reported earlier for normal fibroblasts [47].

Together with immune cells, fibroblasts are able to support the survival of the tumor [48,49]. Although many genes involved in signaling pathways for growth factors (*i.e.* EGF/EGFR) have been identified in CAFs [48-51], a differential expression of these particular growth factors or receptors has not been observed by us. Interestingly, two members of the epidermal growth factor (EGF) family downstream of the EGF receptor pathway have been found with increased expression in irradiated CAFs: the autocrine growth factor and mitogen for fibroblasts amphiregulin (AREG), and epidermal growth factor receptor pathway substrate 8-related protein 2 (EPS8L2). Increased expression of AREG might have an effect on

tumor growth since it has been shown that AREG can inhibit growth and apoptosis in certain aggressive adenoma cell lines in culture [52]. However, increased expression of EPS8 has been linked to progression of squamous carcinogenesis and might confer pro-tumorigenic effects on the surrounding tumor tissue [53]. It is therefore tempting to speculate that alternative signaling mechanisms may deregulate EGFR signaling during carcinogenesis, such as over-expression or activation of EGF/EGFR pathway intermediates.

CAFs express extracellular matrix (ECM) proteins and matrix regulatory agents, thereby providing a favourable microenvironment for cancer cells which is followed by a stimulation of proliferation of tumors and metastasis [54-56]. The increased expression of collagen type VII, alpha COL7A1 might sustain the stability of the cellular organization within the tumor microenvironment by contributing to epithelial basement membrane organization and adherence by interacting with ECM proteins. On the other hand, the matrix metalloproteinase 11 (stromelysin 3) (MMP11) is the solely significant differentially expressed matrix metalloproteinase after irradiation. The enhanced expression of MMP11 in CAFs could promote cancer progression by remodeling the ECM and confers anti-apoptotic and anti-necrotic effects on tumor cells [57]. Numerous studies have linked increased MMP11 expression in different human cancers with poor disease prognosis [58,59], and have been recently suggested to represent a new prognostic indicator for gastric cancer [60]. In addition, the ECM protein Gla protein (MGP) showed decreased expression which can be associated with poor prognosis of lung cancer as has been recently reported for colorectal adenocarcinoma [61]. A potential role for MGP as a prognostic marker for breast cancer has also been implied [62]. Increased expression levels of multiple splice variants for neuregulin-1 (NRG1) in CAFs (see also **Supplemental list 1**) might have an impact on neighboring epithelial cells by inducing their growth and differentiation [63,64]. Elevated expression of gasdermin B (GSDMB) imply a regulatory role for irradiated CAFs on the adjacent epithelial cells, as augmented expression of GSDML has been correlated to cancer progression in the gastric epithelium [65].

In conclusion, CAFs are able to survive ablative radiation doses, but such insult provoke prominent cellular damages and consequently numerous genes implicated in DNA repair, cellular stress and cell survival pathways are activated. Our analyses show that CAFs display both pro- and anti-tumorigenic effects after having received a single high-dose of ionizing radiation. These effects might have an impact on the tumor microenvironment in respect to tumor growth and metastasis. The complexity of the observed differential gene expression patterns and

implicative biological effects are interesting future objectives for further elucidations.

5. Acknowledgements

Funding was provided by the North Norway Regional Health Authority (Helse Nord) and Aakre Foundation. Microarray experiments were conducted at the Microarray Resource Centre Tromsø (MRCT), which is supported by the National Program for Research and Functional Genomics in Norway (FUGE), University of Tromsø and University Hospital North Norway. The authors have no potential conflicts of interest to disclose.

REFERENCES

- [1] J. H. Heinzerling, B. Kavanagh and R. D. Timmerman, "Stereotactic Ablative Radiation Therapy for Primary Lung Tumors," *Cancer Journal*, Vol. 17, No. 1, 2011, pp. 28-32. [doi:10.1097%2FPPPO.0b013e31820a7f80](https://doi.org/10.1097%2FPPPO.0b013e31820a7f80)
- [2] D. Palma and S. Senan, "Stereotactic Radiation Therapy: Changing Treatment Paradigms for Stage I Non Small Cell Lung Cancer," *Current Opinion in Oncology*, Vol. 23, No. 2, 2011, pp. 133-139. [doi:10.1097%2FFCCO.0b013e328341ee11](https://doi.org/10.1097%2FFCCO.0b013e328341ee11)
- [3] B. D. Kavanagh, M. Miften and R. A. Rabinovitch, "Advances in Treatment Techniques: Stereotactic Body Radiation Therapy and the Spread of Hypofractionation," *Cancer Journal*, Vol. 17, No. 3, 2011, pp. 177-181. [doi:10.1097%2FPPPO.0b013e31821f7dbd](https://doi.org/10.1097%2FPPPO.0b013e31821f7dbd)
- [4] T. B. Lanni Jr., I. S. Grills, L. L. Kestin and J. M. Robertson, "Stereotactic Radiotherapy Reduces Treatment Cost while Improving Overall Survival and Local Control over Standard Fractionated Radiation Therapy for Medically Inoperable Non-Small-Cell Lung Cancer," *American Journal of Clinical Oncology*, Vol. 34, No. 5, 2011, pp. 494-498. [doi:10.1097%2FCOC.0b013e3181ec63ae](https://doi.org/10.1097%2FCOC.0b013e3181ec63ae)
- [5] M. P. Lisanti, U. E. Martinez-Outschoorn, B. Chiavarina, S. Pavlides, D. Whitaker-Menezes, A. Tsirigos, A. Witkiewicz, Z. Lin, R. Balliet, A. Howell and F. Sotgia, "Understanding the 'Lethal' Drivers of Tumor-Stroma Co-Evolution: Emerging Role(s) for Hypoxia, Oxidative Stress and Autophagy/Mitophagy in the Tumor Micro-Environment," *Cancer Biology and Therapy*, Vol. 10, No. 6, 2010, pp. 537-542. [doi:10.4161%2Fcbt.10.6.13370](https://doi.org/10.4161%2Fcbt.10.6.13370)
- [6] K. Pietras and A. Ostman, "Hallmarks of Cancer: Interactions with the Tumor Stroma," *Experimental Cell Research*, Vol. 316, No. 8, 2010, pp. 1324-1331. [doi:10.1016%2Fj.yexcr.2010.02.045](https://doi.org/10.1016%2Fj.yexcr.2010.02.045)
- [7] M. Allen and J. L. Jones, "Jekyll and Hyde: The Role of the Microenvironment on the Progression of Cancer," *The Journal of Pathology*, Vol. 223, No. 2, 2011, pp. 162-176.
- [8] K. Räsänen and A. Vaheri, "Activation of Fibroblasts in Cancer Stroma," *Experimental Cell Research*, Vol. 316, No. 17, 2010, pp. 2713-2722. [doi:10.1016%2Fj.yexcr.2010.04.032](https://doi.org/10.1016%2Fj.yexcr.2010.04.032)
- [9] E. Kis, T. Szatmari, M. Keszei, R. Farkas, O. Esik, K.

- Lumniczky, A. Falus and G. Safrany, "Microarray Analysis of Radiation Response Genes in Primary Human Fibroblasts," *International Journal of Radiation Oncology, Biology, Physics*, Vol. 66, No. 5, 2006, pp. 1506-1514. [doi:10.1016%2Fj.ijrobp.2006.08.004](https://doi.org/10.1016%2Fj.ijrobp.2006.08.004)
- [10] S. Tachiiri, T. Katagiri, T. Tsunoda, N. Oya, M. Hiraoka and Y. Nakamura, "Analysis of Gene-Expression Profiles after Gamma Irradiation of Normal Human Fibroblasts," *International Journal of Radiation Oncology, Biology, Physics*, Vol. 64, No. 1, 2006, pp. 272-279. [doi:10.1016%2Fj.ijrobp.2005.08.030](https://doi.org/10.1016%2Fj.ijrobp.2005.08.030)
- [11] O. K. Rødningen, J. Øvergaard, J. Alsner, T. Hastie and A. L. Børresen-Dale, "Microarray Analysis of the Transcriptional Response to Single or Multiple Doses of Ionizing Radiation in Human Subcutaneous Fibroblasts," *Radiotherapy and Oncology*, Vol. 77, No. 3, 2005, pp. 231-240. [doi:10.1186%2Fbcr1151](https://doi.org/10.1186%2Fbcr1151)
- [12] H. Landmark, S. A. Nahas, J. Aaroe, R. Gatti, A. L. Børresen-Dale and O. K. Rødningen, "Transcriptional Response to Ionizing Radiation in Human Radiation Sensitive Cell Lines," *Radiotherapy and Oncology*, Vol. 83, No. 3, 2007, pp. 256-260.
- [13] O. K. Rødningen, A. L. Børresen-Dale, J. Alsner, T. Hastie and J. Øvergaard, "Radiation-Induced Gene Expression in Human Subcutaneous Fibroblasts is Predictive of Radiation-Induced Fibrosis," *Radiotherapy and Oncology*, Vol. 86, No. 3, 2008, pp. 314-320. [doi:10.1016%2Fj.radonc.2007.09.013](https://doi.org/10.1016%2Fj.radonc.2007.09.013)
- [14] T. Hellevik, I. Pettersen, V. Berg, J. O. Winberg, B. T. Moe, K. Bartnes, R. H. Paulssen, L. T. Busund, R. Bremnes, A. Chalmers and I. Martinez-Zubiaurre, "Cancer-Associated Fibroblasts from Human NSCLC Survive Ablative Doses of Radiation but Their Invasive Capacity is Reduced," *Radiation Oncology*, Vol. 7, No. 1, 2012, pp. 59-71. [doi:10.1186%2F1748-717X-7-59](https://doi.org/10.1186%2F1748-717X-7-59)
- [15] S. Stathakis, J. S. Li, K. Paskalev, J. Yang, L. Wang and C. M. Ma, "Ultra-Thin TLDs for Skin Dose Determination in High Energy Photon Beams," *Physics in Medicine and Biology*, Vol. 51, No. 14, 2006, pp. 3549-3567. [doi:10.1088%2F0031-9155%2F51%2F14%2F018](https://doi.org/10.1088%2F0031-9155%2F51%2F14%2F018)
- [16] T. Mosmann, "Rapid Colorimetric Assay for Cellular Growth and Survival: Application to Proliferation and Cytotoxicity Assays," *Journal of Immunological Methods*, Vol. 65, No. 1-2, 1983, pp. 55-63. [doi:10.1016%2F0022-1759%2883%2990303-4](https://doi.org/10.1016%2F0022-1759%2883%2990303-4)
- [17] R. H. Paulssen, L. Olsen and T. C. Sogn, "MagNa Pure Compact RNA Isolation Kit: Isolation of High-Quality Total RNA from a Broad Range of Sample Material," *Biochimica*, Vol. 2, 2006, pp. 14-16.
- [18] B. M. Bolstad, R. A. Irizarry, M. Astrand and T. P. Speed, "A Comparison of Normalization Methods for High Density Oligonucleotide Array Data Based on Variance and Bias," *Bioinformatics*, Vol. 19, No. 2, 2003, pp. 185-193. [doi:10.1093%2Fbioinformatics%2F19.2.185](https://doi.org/10.1093%2Fbioinformatics%2F19.2.185)
- [19] G. K. Smyth, "Linear Models and Empirical Bayes Methods for Assessing Differential Expression in Microarray Experiments," *Statistical Applications in Genetics and Molecular Biology*, Vol. 3, No. 1, 2004, pp. 1544-6115. [doi:10.2202%2F1544-6115.1027](https://doi.org/10.2202%2F1544-6115.1027)
- [20] Y. Benjamini and D. Yekutieli, "False Discovery Rate-Adjusted Multiple Confidence Intervals for Selected Parameters," *Journal of the American Statistical Association*, Vol. 100, No. 469, 2005, pp. 71-81. [doi:10.1198%2F016214504000001907](https://doi.org/10.1198%2F016214504000001907)
- [21] L. Gidskehaug, H. Stodkilde-Jorgensen, M. Martens and H. Martens, "Bridge-PLS Regression: Two-Block Bilinear Regression without Deflation," *Journal of Chemometrics*, Vol. 18, No. 3-4, 2004, pp. 208-215. [doi:10.1002%2Fcem.862](https://doi.org/10.1002%2Fcem.862)
- [22] K. J. Livak and T. D. Schmittgen, "Analysis of Relative Gene Expression Data using Real-Time Quantitative PCR and The 2(-Delta Delta C(T)) Method," *Methods*, Vol. 25, No. 4, 2001, pp. 402-408.
- [23] G. Li and D. Reinberg, "Chromatin Higher-Order Structures and Gene Regulation," *Current Opinion in Genetics & Development*, Vol. 21, No. 2, 2011, pp. 175-186. [doi:10.1016%2Fj.gde.2011.01.022](https://doi.org/10.1016%2Fj.gde.2011.01.022)
- [24] A. Krtolica, S. Parrinello, S. Lockett, P. Y. Desprez and J. Campisi, "Senescent Fibroblasts Promote Epithelial Cell Growth and Tumorigenesis: A Link Between Cancer and Aging," *Proceedings of the National Academy of Sciences of the United States of America*, Vol. 98, No. 21, 2001, pp. 12072-12077. [doi:10.1073%2Fpnas.211053698](https://doi.org/10.1073%2Fpnas.211053698)
- [25] J. L. Wang and P. C. Wang, "The Effect of Aging on the DNA Damage and Repair Capacity in 2BS Cells Undergoing Oxidative Stress," *Molecular Biology Reports*, Vol. 39, No. 1, 2012, pp. 233-241. [doi:10.1007%2Fs11033-011-0731-4](https://doi.org/10.1007%2Fs11033-011-0731-4)
- [26] C. Bavik, I. Coleman, J. P. Dean, B. Knudsen, S. Plymate and P. S. Nelson, "The Gene Expression Program of Prostate Fibroblast Senescence Modulates Neoplastic Epithelial Cell Proliferation through Paracrine Mechanisms," *Cancer Research*, Vol. 66, No. 2, 2006, pp. 794-802. [doi:10.1158%2F0008-5472.CAN-05-1716](https://doi.org/10.1158%2F0008-5472.CAN-05-1716)
- [27] T. B. Kryston, A. B. Georgiev, P. Pissis and A. G. Georgakilas, "Role of Oxidative Stress and DNA Damage in Human Carcinogenesis," *Mutation Research*, Vol. 711, No. 1-2, 2011, pp. 193-201. [doi:10.1016%2Fj.mrfmmm.2010.12.016](https://doi.org/10.1016%2Fj.mrfmmm.2010.12.016)
- [28] P. L. Miliani de Marval and Y. Zhang, "The RP-Mdm2-p53 Pathway and Tumorigenesis," *Oncotarget*, Vol. 2, No. 3, 2011, pp. 234-238.
- [29] J. J. Manfredi, "The Mdm2-p53 Relationship Evolves: Mdm2 Swings Both Ways as an Oncogene and a Tumor Suppressor," *Genes & Development*, Vol. 24, No. 15, 2010, pp. 1580-1589. [doi:10.1101%2Fgad.1941710](https://doi.org/10.1101%2Fgad.1941710)
- [30] L. C. Harris, "MDM2 Splice Variants and Their Therapeutic Implications," *Current Cancer Drug Targets*, Vol. 5, No. 1, 2005, pp. 21-26. [doi:10.2174%2F1568009053332654](https://doi.org/10.2174%2F1568009053332654)
- [31] K. Ogawa, S. Murayama and M. Mori, "Predicting the Tumor Response to Radiotherapy Using Microarray Analysis," *Oncology Reports*, Vol. 18, No. 5, 2007, pp. 1243-1248.
- [32] W. F. Guo, R. X. Lin, J. Huang, Z. Zhou, J. Yang, G. Z.

- Guo and S. Q. Wang, "Identification of Differentially Expressed Genes Contributing to Radioresistance in Lung Cancer Cells Using Microarray Analysis," *Radiation Research*, Vol. 164, No. 1, 2005, pp. 27-35.
[doi:10.1667%2FR3401](https://doi.org/10.1667%2FR3401)
- [33] U. E. Martinez-Outschoorn, S. Pavlides, A. Howell, R. G. Pestell, H. B. Tanowitz, F. Sotgia and M. P. Lisanti, "Stromal-Epithelial Metabolic Coupling in Cancer: Integrating Autophagy and Metabolism in the Tumor Microenvironment," *The International Journal of Biochemistry & Cell Biology*, Vol. 43, No. 7, 2011, pp. 1045-1051.
[doi:10.1016%2Fj.biocel.2011.01.023](https://doi.org/10.1016%2Fj.biocel.2011.01.023)
- [34] H. Chaachouay, P. Ohneseit, M. Toulany, R. Kehlbach, G. Multhoff and H. P. Rodemann, "Autophagy Contributes to Resistance of Tumor Cells to Ionizing Radiation," *Radiotherapy and Oncology*, Vol. 99, No. 3, 2011, pp. 287-292. [doi:10.1016%2Fj.radonc.2011.06.002](https://doi.org/10.1016%2Fj.radonc.2011.06.002)
- [35] M. Ao, O. E. Franco, D. Park, D. Raman, K. Williams and S. W. Hayward, "Cross-Talk between Paracrine-Acting Cytokine and Chemokine Pathways Promotes Malignancy in Benign Human Prostatic Epithelium," *Cancer Research*, Vol. 67, No. 9, 2007, pp. 4244-4253.
[doi:10.1158%2F0008-5472.CAN-06-3946](https://doi.org/10.1158%2F0008-5472.CAN-06-3946)
- [36] R. F. Hwang, T. Moore, T. Arumugam, V. Ramachandran, K. D. Amos, A. Rivera, B. Ji, D. B. Evans and C. D. Logsdon, "Cancer-Associated Stromal Fibroblasts Promote Pancreatic Tumor Progression," *Cancer Research*, Vol. 68, No. 3, 2008, pp. 918-926.
[doi:10.1158%2F0008-5472.CAN-07-5714](https://doi.org/10.1158%2F0008-5472.CAN-07-5714)
- [37] A. D. Blann, K. S. Ramcharan, P. S. Stonelake, D. Luesley and G. Y. Lip, "The Angiome: A New Concept in Cancer Biology," *Journal of Clinical Pathology*, Vol. 64, No. 7, 2011, pp. 637-643.
[doi:10.1136%2Fjcp.2011.088948](https://doi.org/10.1136%2Fjcp.2011.088948)
- [38] J. M. Ko, P. L. Chan, W. L. Yau, H. K. Chan, K. C. Chan, Z. Y. Yu, F. M. Kwong, L. D. Miller, E. T. Liu, L. C. Yang, P. H. Lo, E. J. Stanbridge, J. C. Tang, G. Srivastava, S. W. Tsao, S. Law and M. L. Lung, "Monochromosome Transfer and Microarray Analysis Identify a Critical Tumor-Suppressive Region Mapping to Chromosome 13q14 and THSD1 in Esophageal Carcinoma," *Molecular Cancer Research*, Vol. 6, No. 4, 2008, pp. 592-603. [doi:10.1158%2F1541-7786.MCR-07-0154](https://doi.org/10.1158%2F1541-7786.MCR-07-0154)
- [39] L. C. Armstrong and P. Bornstein, "Thrombospondins 1 and 2 Function as Inhibitors of Angiogenesis," *Matrix Biology*, Vol. 22, No. 1, 2003, pp. 63-71.
[doi:10.1016%2F0945-053X%2803%2900005-2](https://doi.org/10.1016%2F0945-053X%2803%2900005-2)
- [40] P. Bornstein, "Thrombospondins Function as Regulators of Angiogenesis," *Journal of Cell Communication and Signaling*, Vol. 3, No. 3-4, 2009, pp. 189-200.
[doi:10.1007%2Fs12079-009-0060-8](https://doi.org/10.1007%2Fs12079-009-0060-8)
- [41] F. de Fraipont, A. C. Nicholson, J. J. Feige and E. G. Van Meir, "Thrombospondins and Tumor Angiogenesis," *Trends in Molecular Medicine*, Vol. 7, No. 9, 2001, pp. 401-407.
[doi:10.1016%2F1471-4914%2801%2902102-5](https://doi.org/10.1016%2F1471-4914%2801%2902102-5)
- [42] F. Cavallo, E. Quaglino, L. Cifaldi, E. Di Carlo, A. Andre, P. Bernabei, P. Musiani, G. Forni and R. A. Calogero, "Interleukin 12-Activated Lymphocytes Influence Tumor Genetic Programs," *Cancer Research*, Vol. 61, No. 8, 2001, pp. 3518-3523.
- [43] A. Sakurai, C. Doci and J. S. Gutkind, "Semaphorin Signaling in Angiogenesis, Lymphangiogenesis and Cancer," *Cell Research*, Vol. 22, No. 1, 2012, pp. 23-32.
[doi:10.1038%2Fcr.2012.21](https://doi.org/10.1038%2Fcr.2012.21)
- [44] T. Ito, M. Kagoshima, Y. Sasaki, C. Li, N. Udaka, T. Kitsukawa, H. Fujisawa, M. Taniguchi, T. Yagi, H. Kitamura and Y. Goshima, "Repulsive Axon Guidance Molecule Sema3A Inhibits Branching Morphogenesis of Fetal Mouse Lung," *Mechanisms of Development*, Vol. 97, No. 1-2, 2000, pp. 35-45.
[doi:10.1016%2FS0925-4773%2800%2900401-9](https://doi.org/10.1016%2FS0925-4773%2800%2900401-9)
- [45] M. Kagoshima and T. Ito, "Diverse Gene Expression and Function of Semaphorins in Developing Lung: Positive and Negative Regulatory Roles of Semaphorins in Lung Branching Morphogenesis," *Genes to Cells: Devoted to Molecular and Cellular Mechanisms*, Vol. 6, No. 6, 2001, pp. 559-571. [doi:10.1046%2Fj.1365-2443.2001.00441.x](https://doi.org/10.1046%2Fj.1365-2443.2001.00441.x)
- [46] V. A. Potiron, J. Roche and H. A. Drabkin, "Semaphorins and Their Receptors in Lung Cancer," *Cancer Letters*, Vol. 273, No. 1, 2009, pp. 1-14.
[doi:10.1016%2Fj.canlet.2008.05.032](https://doi.org/10.1016%2Fj.canlet.2008.05.032)
- [47] D. Barberis, S. Artigiani, A. Casazza, S. Corso, S. Giordano, C. A. Love, E. Y. Jones, P. M. Comoglio and L. Tamagnone, "Plexin Signaling Hampers Integrin-Based Adhesion, Leading to Rho-Kinase Independent Cell Rounding, and Inhibiting Lamellipodia Extension and Cell Motility," *FASEB Journal*, Vol. 18, No. 3, 2004, pp. 592-594.
- [48] N. A. Bhowmick, E. G. Neilson and H. L. Moses, "Stromal Fibroblasts in Cancer Initiation and Progression," *Nature*, Vol. 432, No. 7015, 2004, pp. 332-337.
[doi:10.1038%2Fnature03096](https://doi.org/10.1038%2Fnature03096)
- [49] M. Akdis, S. Burgler, R. Cramer, T. Eiwegger, H. Fujita, E. Gomez, S. Klunker, N. Meyer, L. O'Mahony, O. Palomares, C. Rhyner, N. Ouaked, A. Schaffartzik, W. Van De Veen, S. Zeller, M. Zimmermann and C. A. Akdis, "Interleukins, from 1 to 37, and Interferon-Gamma: Receptors, Functions, and Roles in Diseases," *The Journal of Allergy and Clinical Immunology*, Vol. 127, No. 3, 2011, pp. 701-721. [doi:10.1016%2Fj.jaci.2010.11.050](https://doi.org/10.1016%2Fj.jaci.2010.11.050)
- [50] R. Kalluri and M. Zeisberg, "Fibroblasts in Cancer," *Nature Reviews. Cancer*, Vol. 6, No. 5, 2006, pp. 392-401.
[doi:10.1038%2Fnrc1877](https://doi.org/10.1038%2Fnrc1877)
- [51] H. Nakagawa, S. Liyanarachchi, R. V. Davuluri, H. Auer, E. W. Martin Jr., A. de la Chapelle and W. L. Frankel, "Role of Cancer-Associated Stromal Fibroblasts in Metastatic Colon Cancer to the Liver and Their Expression Profiles," *Oncogene*, Vol. 23, No. 44, 2004, pp. 7366-7377. [doi:10.1038%2Fsj.onc.1208013](https://doi.org/10.1038%2Fsj.onc.1208013)
- [52] A. Hurbin, L. Dubrez, J. L. Coll and M. C. Favrot, "Inhibition of Apoptosis by Amphiregulin via an Insulin-Like Growth Factor-1 Receptor-Dependent Pathway in Non-Small Cell Lung Cancer Cell Lines," *The Journal of Biological Chemistry*, Vol. 277, No. 51, 2002, pp. 49127-49133. [doi:10.1074%2Fjbc.M207584200](https://doi.org/10.1074%2Fjbc.M207584200)

- [53] H. Wang, V. Patel, H. Miyazaki, J. S. Gutkind and W. A. Yeudall, "Role for EPS8 in Squamous Carcinogenesis," *Carcinogenesis*, Vol. 30, No. 1, 2009, pp. 165-174. [doi:10.1016%2Fj.oos.2009.06.212](https://doi.org/10.1016%2Fj.oos.2009.06.212)
- [54] J. A. Joyce and J. W. Pollard, "Microenvironmental Regulation of Metastasis," *Nature Reviews. Cancer*, Vol. 9, No. 4, 2009, pp. 239-252.
- [55] M. Liu, J. Xu and H. Deng, "Tangled Fibroblasts in Tumor-Stroma Interactions," *International Journal of Cancer*, Vol. 129, No. 8, 2011, pp. 1795-1805. [doi:10.1002%2Fijc.26116](https://doi.org/10.1002%2Fijc.26116)
- [56] L. E. Littlepage, M. D. Sternlicht, N. Rougier, J. Phillips, E. Gallo, Y. Yu, K. Williams, A. Brenot, J. I. Gordon and Z. Werb, "Matrix Metalloproteinases Contribute Distinct Roles in Neuroendocrine Prostate Carcinogenesis, Metastasis, and Angiogenesis Progression," *Cancer Research*, Vol. 70, No. 6, 2010, pp. 2224-2234. [doi:10.1158%2F0008-5472.CAN-09-3515](https://doi.org/10.1158%2F0008-5472.CAN-09-3515)
- [57] P. Basset, C. Wolf and P. Chambon, "Expression of the Stromelysin-3 Gene in Fibroblastic Cells of Invasive Carcinomas of the Breast and Other Human Tissues: A Review," *Breast Cancer Research and Treatment*, Vol. 24, No. 3, 1993, pp. 185-193. [doi:10.1007%2FBF01833259](https://doi.org/10.1007%2FBF01833259)
- [58] D. Peruzzi, F. Mori, A. Conforti, D. Lazzaro, E. De Rinaldis, G. Ciliberto, N. La Monica and L. Aurisicchio, "MMP11: A Novel Target Antigen for Cancer Immunotherapy," *Clinical Cancer Research*, Vol. 15, No. 12, 2009, pp. 4104-4113. [doi:10.1158%2F1078-0432.CCR-08-3226](https://doi.org/10.1158%2F1078-0432.CCR-08-3226)
- [59] C. W. Cheng, J. C. Yu, H. W. Wang, C. S. Huang, J. C. Shieh, Y. P. Fu, C. W. Chang, P. E. Wu and C. Y. Shen, "The Clinical Implications of MMP-11 and CK-20 Expression in Human Breast Cancer," *Clinica Chimica Acta*, Vol. 411, No. 3-4, 2010, pp. 234-241. [doi:10.1016%2Fj.cca.2009.11.009](https://doi.org/10.1016%2Fj.cca.2009.11.009)
- [60] Z. S. Zhao, Y. Q. Chu, Z. Y. Ye, Y. Y. Wang and H. Q. Tao, "Overexpression of Matrix Metalloproteinase 11 in Human Gastric Carcinoma and Its Clinicopathologic Significance," *Human Pathology*, Vol. 41, No. 5, 2010, pp. 686-696. [doi:10.1016%2Fj.humpath.2009.10.010](https://doi.org/10.1016%2Fj.humpath.2009.10.010)
- [61] C. Fan, D. Sheu, H. Fan, K. Hsu, C. Allen Chang and E. Chan, "Down-Regulation of Matrix Gla Protein Messenger RNA in Human Colorectal Adenocarcinomas," *Cancer Letters*, Vol. 165, No. 1, 2001, pp. 63-69. [doi:10.1016%2FS0304-3835%2801%2900416-5](https://doi.org/10.1016%2FS0304-3835%2801%2900416-5)
- [62] K. Yoshimura, K. Takeuchi, K. Nagasaki, S. Ogishima, H. Tanaka, T. Iwase, F. Akiyama, Y. Kuroda and Y. Miki, "Prognostic Value of Matrix Gla Protein in Breast Cancer," *Molecular Medicine Reports*, Vol. 2, No. 4, 2009, pp. 549-553. [doi:10.3892%2Fmmr.00000135](https://doi.org/10.3892%2Fmmr.00000135)
- [63] J. C. Montero, R. Rodriguez-Barrueco, A. Ocana, E. Diaz-Rodriguez, A. Esparis-Ogando and A. Pandiella, "Neuregulins and Cancer," *Clinical Cancer Research*, Vol. 14, No. 11, 2008, pp. 3237-3241. [doi:10.1158%2F1078-0432.CCR-07-5133](https://doi.org/10.1158%2F1078-0432.CCR-07-5133)
- [64] N. V. Hayes and W. J. Gullick, "The Neuregulin Family of Genes and Their Multiple Splice Variants in Breast Cancer," *Journal of Mammary Gland Biology and Neoplasia*, Vol. 13, No. 2, 2008, pp. 205-214. [doi:10.1007%2Fs10911-008-9078-4](https://doi.org/10.1007%2Fs10911-008-9078-4)
- [65] H. Komiyama, A. Aoki, S. Tanaka, H. Maekawa, Y. Kato, R. Wada, T. Maekawa, M. Tamura and T. Shiroishi, "Alu-Derived Cis-Element Regulates Tumorigenesis-Dependent Gastric Expression of GASDERMIN B (GSDMB)," *Genes & Genetic Systems*, Vol. 85, No. 1, 2010, pp. 75-83. [doi:10.1266%2Fggs.85.75](https://doi.org/10.1266%2Fggs.85.75)

Supplement

Supplemental list 1. Differentially expressed genes in irradiated cancer-associated fibroblasts.

abi	gene	p value	adjusted p value	fold	diff
NM_138763	BAX	1.81E-009	8.17E-005	0.768024	1.702935451
NM_198947	FAM111B	1.02E-007	0.002286929	-2.58423	-5.996961141
BC024648	PHPT1	2.72E-007	0.003977702	0.684596	1.607251359
AL137582	BAG3	3.53E-007	0.003977702	0.775614	1.711918429
NM_013960	NRG1	5.27E-007	0.004743616	2.464606	5.519760939
BC107485	NEURL2	8.86E-007	0.006652829	1.363829	2.5736732
NM_000882	IL12A	1.18E-006	0.007551732	1.619253	3.072159968
NM_005393	PLXNB3	1.44E-006	0.007551732	1.761463	3.390418511
NM_014010	ASTN2	1.52E-006	0.007551732	1.446603	2.725654531
NM_182649	PCNA	1.95E-006	0.007551732	1.728062	3.312825093
BC012163	MRPL53	2.05E-006	0.007551732	0.626831	1.544169132
NM_003512	HIST1H2AC	2.30E-006	0.007551732	0.853099	1.806377242
NM_006014	XX-FW81657B9.4	2.40E-006	0.007551732	0.877515	1.837208096
NM_005762	TRIM28	2.40E-006	0.007551732	0.477001	1.391847027
NM_015657	ABCA12	2.52E-006	0.007551732	1.634961	3.105792397
NM_002756	MAP2K3	3.28E-006	0.009231482	0.573737	1.488373917
NM_198188	ASTN2	3.51E-006	0.009303796	1.82306	3.538308168
BC065913	ASB6	4.24E-006	0.010612757	0.809592	1.752715705
BC053682	COTL1	4.54E-006	0.010752587	0.565244	1.479637227
BC032503	ANAPC2	5.46E-006	0.011440042	0.969125	1.957652542
NM_000251	MSH2	5.90E-006	0.011440042	-0.5434	-1.457400956
NM_013958	NRG1	6.29E-006	0.011440042	2.788939	6.911211173
XM_928391	LOC653611	6.48E-006	0.011440042	1.046302	2.065229185
NM_032431	SYVN1	6.73E-006	0.011440042	0.625822	1.543089849
BC007015	CCNE2	6.99E-006	0.011440042	-2.15266	-4.446476235
NM_133172	APBB3	7.07E-006	0.011440042	0.703604	1.628568141
BC003080	HSPC171	7.30E-006	0.011440042	0.655253	1.574892306
NM_006271	S100A1	7.71E-006	0.011440042	0.716574	1.643275218
NM_001014987	LAT	7.72E-006	0.011440042	0.896101	1.861029934
BC108737	HIST1H2BK	7.72E-006	0.011440042	1.345575	2.541314945
AK026810	TAF7L	8.14E-006	0.011440042	2.562542	5.907477687
AK057029	HTF9C	8.23E-006	0.011440042	0.686178	1.609015677
NM_181738	PRDX2	8.44E-006	0.011440042	0.463577	1.378956969
BC005896	HYAL3	8.64E-006	0.011440042	1.320064	2.496772504

Continued

NM_006878	MDM2	9.39E-006	0.01177774	1.222556	2.333598241
BC092487	ASAH3L	9.42E-006	0.01177774	1.740934	3.342516066
NM_033388	ATG16L2	1.01E-005	0.01202843	0.924626	1.898191986
NM_006232	POLR2H	1.01E-005	0.01202843	0.700125	1.624645442
BC101544	GRIPAP1	1.10E-005	0.012696458	0.719984	1.647163924
AF385325	MDM2	1.13E-005	0.012696458	1.387494	2.61623886
NM_013962	NRG1	1.19E-005	0.012840948	2.424391	5.368023002
NM_002392	MDM2	1.20E-005	0.012840948	0.933639	1.910088158
NM_002434	MPG	1.35E-005	0.014091567	0.631122	1.548768522
BC000298	NINJ1	1.43E-005	0.014647145	1.003179	2.004411248
AK023030	JMJD4	1.54E-005	0.015141866	0.717407	1.644224074
BC013685	MRPL2	1.55E-005	0.015141866	0.604732	1.520696638
BC011762	CYFIP2	1.62E-005	0.015558825	2.040759	4.114618331
NM_001254	CDC6	1.67E-005	0.015635117	-1.65638	-3.152240503
XM_929083	LOC653319	1.78E-005	0.015950766	0.65515	1.574779228
BC018722	ASPSR1	1.79E-005	0.015950766	0.49265	1.407027358
NM_013964	NRG1	1.87E-005	0.015950766	2.052564	4.148427122
XM_929687	LOC646739	1.90E-005	0.015950766	2.057284	4.162020136
NM_004110	FDXR	1.91E-005	0.015950766	2.181207	4.535328896
AF385327	MDM2	1.93E-005	0.015950766	1.089126	2.127451263
BC070493	TOB1	1.95E-005	0.015950766	0.757875	1.690997951
NM_015655	ZNF337	2.06E-005	0.016199911	0.762378	1.696284223
CR592601	HTF9C	2.06E-005	0.016199911	0.743771	1.674546788
AF370432	PML	2.09E-005	0.016199911	0.459983	1.375525262
NM_003172	SURF1	2.12E-005	0.016199911	0.730661	1.659399508
AK125827	LRRC41	2.23E-005	0.016736193	0.256379	1.194477114
BC002649	HIST1H1C	2.33E-005	0.01697618	1.161077	2.236243048
BC031558	C1orf183	2.37E-005	0.01697618	1.386175	2.613848298
XM_934793	DENND4B	2.43E-005	0.01697618	0.38942	1.309866399
BC007518	HIST1H3H	2.44E-005	0.01697618	1.4268	2.688497932
NM_000094	COL7A1	2.45E-005	0.01697618	1.604835	3.041610634
BC067436	CYP3A7	2.52E-005	0.01717885	1.596736	3.024581609
NM_013956	NRG1	2.64E-005	0.017765058	2.53177	5.782807855
M80185	PML	2.69E-005	0.017793919	0.673749	1.595213097
AK001070	ZNF692	2.73E-005	0.017793919	0.768237	1.703186724
BC041667	EYA3	2.87E-005	0.018025584	-0.54224	-1.456230612

Continued

NM_001025593	ARFIP1	2.89E-005	0.018025584	-0.52497	-1.43890505
NM_033200	BC002942	2.90E-005	0.018025584	0.659475	1.579507307
AF064771	DGKA	2.95E-005	0.018025584	0.846342	1.797937033
BC005091	HERPUD2	2.97E-005	0.018025584	-0.47142	-1.386468691
NM_004628	XPC	3.07E-005	0.018025584	0.828717	1.776105322
AF385322	MDM2	3.11E-005	0.018025584	1.030412	2.042608064
BC003099	DPH1	3.12E-005	0.018025584	0.707869	1.633390081
BC028337	GCS1	3.15E-005	0.018025584	0.503381	1.417531968
NM_002486	NCBP1	3.16E-005	0.018025584	-0.35423	-1.2783016
AF385323	MDM2	3.26E-005	0.018157822	1.279149	2.426957431
NM_032324	C1orf57	3.27E-005	0.018157822	0.66364	1.584073802
BC070314	MGP	3.32E-005	0.018239392	-0.77447	-1.710559503
AK091661	DCTN3	3.45E-005	0.018727419	0.867575	1.824592969
NM_020375	C12orf5	3.51E-005	0.018833349	1.140114	2.203983739
NM_017445	H2BFS	3.72E-005	0.01972195	0.734732	1.664087997
BC019269	MRPL16	3.83E-005	0.020044557	0.069647	1.049460059
NM_001039476	C16orf35	3.88E-005	0.020094339	0.631713	1.54940335
CR605682	LYPLA2	4.02E-005	0.020402425	0.796434	1.736803381
NM_025165	ELL3	4.03E-005	0.020402425	0.621991	1.538997666
AF054506	SLC12A4	4.19E-005	0.0206016	0.741354	1.671743996
NM_182706	SCRIB	4.19E-005	0.0206016	1.133978	2.194630675
CR598294	C1orf66	4.21E-005	0.0206016	0.821877	1.767704092
NM_130459	TOR2A	4.25E-005	0.0206016	0.78156	1.718989092
AK123386	unknown	4.40E-005	0.020604536	0.837939	1.787495266
NM_032885	ATG4D	4.45E-005	0.020604536	0.534127	1.448065937
BC062362	RPUSD3	4.45E-005	0.020604536	0.629028	1.546522703
BC110622	LIG1	4.57E-005	0.020604536	1.233335	2.351099013
NM_005632	SOLH	4.68E-005	0.020604536	0.554222	1.468376578
NM_005223	DNASE1	4.69E-005	0.020604536	0.462391	1.377823672
NM_024328	THTPA	4.70E-005	0.020604536	0.806855	1.749393213
NM_206920	MAMDC4	4.72E-005	0.020604536	1.063317	2.089730133
XM_934621	LOC284184	4.76E-005	0.020604536	1.02759	2.038616432
NM_013301	HSU79303	4.79E-005	0.020604536	0.726878	1.655054002
AF385324	unknown	5.10E-005	0.020604536	1.604606	3.041125889
BC069473	GGT1	5.11E-005	0.020604536	1.312771	2.484181921
AF176921	unknown	5.11E-005	0.020604536	2.886867	7.39662435

Continued

NM_145059	FUK	5.15E-005	0.020604536	1.000631	2.000874678
NM_017722	TRMT1	5.23E-005	0.020604536	0.86186	1.817380484
XM_930513	LOC440456	5.34E-005	0.020604536	0.764318	1.6985666
BC039024	FBXO22	5.43E-005	0.020604536	0.876871	1.836388403
BC069418	CYP3A4	5.45E-005	0.020604536	1.675782	3.194925896
NM_015209	RP1-21O18.1	5.51E-005	0.020604536	0.603114	1.518991706
AK127080	LZTR1	5.59E-005	0.020604536	0.49886	1.413096403
NM_012170	FBXO22	5.62E-005	0.020604536	1.194935	2.289345202
NM_022767	ISG20L1	5.64E-005	0.020604536	0.726529	1.654652821
NM_000613	HPX	5.64E-005	0.020604536	1.330857	2.515521393
NM_017905	TMCO3	5.68E-005	0.020604536	-0.41016	-1.328837059
NM_004328	BCS1L	5.69E-005	0.020604536	0.608159	1.524312942
NM_007150	ZNF185	5.70E-005	0.020604536	0.577086	1.491833043
AL834398	LSM14A	5.72E-005	0.020604536	-0.36327	-1.2863396
AK055777	FLYWCH1	5.73E-005	0.020604536	0.544903	1.458922371
NM_003869	CES2	5.80E-005	0.020604536	0.986578	1.981479327
NM_003917	APIG2	5.83E-005	0.020604536	0.658535	1.578478896
AY930112	DGKA	5.86E-005	0.020604536	1.163852	2.240548918
NM_006881	MDM2	5.88E-005	0.020604536	1.408208	2.654072044
BC006523	SGK2	5.92E-005	0.020604536	-1.36108	-2.568780585
BC002882	C16orf5	5.92E-005	0.020604536	0.540191	1.454165515
NM_000903	NQO1	5.94E-005	0.020604536	-0.59173	-1.507057308
XM_932518	LOC644923	5.99E-005	0.020604536	-0.3949	-1.314852061
BC018143	CDC34	5.99E-005	0.020604536	0.453384	1.369248658
NM_006225	PLCD1	6.18E-005	0.020604536	0.906876	1.87498064
BC000491	PCNA	6.46E-005	0.020604536	1.36268	2.571625345
NM_018494	LRDD	6.47E-005	0.020604536	2.041902	4.11788099
AF319947	MMS19	6.49E-005	0.020604536	0.422518	1.340264634
XM_928241	LOC643452	6.49E-005	0.020604536	-0.51581	-1.429800129
NM_004480	FUT8	6.49E-005	0.020604536	-0.51548	-1.42947169
NM_033004	NALP1	6.51E-005	0.020604536	0.833615	1.782145605
XM_933587	LOC643556	6.54E-005	0.020604536	0.610897	1.527208453
NM_003805	CRADD	6.55E-005	0.020604536	0.646205	1.56504606
BC078144	SULT1A4	6.61E-005	0.020604536	0.707714	1.63321418
NM_006019	TCIRG1	6.64E-005	0.020604536	0.363656	1.286682725
NM_033240	PML	6.65E-005	0.020604536	0.531943	1.445874775

Continued

NM_018676	THSD1	6.67E-005	0.020604536	1.405445	2.648995451
BC104992	KIAA1033	6.81E-005	0.020604536	-0.49818	-1.412426327
BC093632	FAAH	6.83E-005	0.020604536	1.1291	2.18722269
NM_015169	RRS1	6.92E-005	0.020604536	0.779009	1.715952137
NM_080749	NEURL2	6.94E-005	0.020604536	1.043313	2.060954583
NM_003534	HIST1H3G	6.98E-005	0.020604536	0.773666	1.709608644
AY359091	ARNT	6.99E-005	0.020604536	-0.49157	-1.4059694
BC105637	OGFOD2	7.08E-005	0.020604536	0.88945	1.85246971
NM_006536	CLCA2	7.13E-005	0.020604536	1.987447	3.965347424
NM_006880	MDM2	7.25E-005	0.020604536	1.140287	2.204248353
XM_928729	LOC645719	7.26E-005	0.020604536	0.483691	1.3983167
NM_017460	CYP3A4	7.30E-005	0.020604536	1.646393	3.130499695
BC069522	RBP2	7.33E-005	0.020604536	1.007376	2.010251338
NM_181573	RFC4	7.33E-005	0.020604536	-0.78187	-1.719360163
NM_006844	ILVBL	7.38E-005	0.020604536	0.376307	1.298014812
BC029360	SUV39H2	7.39E-005	0.020604536	-0.58396	-1.498954432
NM_198576	AGRN	7.43E-005	0.020604536	0.558501	1.472738366
NM_001003692	ZMAT5	7.50E-005	0.020604536	0.83809	1.787681974
NM_013959	NRG1	7.52E-005	0.020604536	2.619473	6.145254462
AM180340	BLNK	7.54E-005	0.020604536	2.706194	6.525976329
NM_005940	MMP11	7.60E-005	0.020604536	1.280345	2.42897061
NM_000666	ACY1	7.69E-005	0.020604536	0.649747	1.56889254
NM_001007523	F8A2	7.71E-005	0.020604536	0.696871	1.620984908
NM_018209	ARFGAP1	7.72E-005	0.020604536	0.459677	1.37523368
AY444560	C8orf38	7.76E-005	0.020604536	1.443874	2.720504354
AY358149	THSD1	7.79E-005	0.020604536	1.508763	2.845658704
AK000538	ZNF692	7.81E-005	0.020604536	0.579584	1.494418065
BC053670	FLJ21736	7.85E-005	0.020604536	2.606133	6.088692786
BC005272	MGP	7.88E-005	0.020604536	-0.77654	-1.713013501
BC009189	NDUFA13	7.91E-005	0.020604536	0.630508	1.548110487
NM_025233	COASY	7.97E-005	0.020604536	0.456961	1.372647484
NM_014278	HSPA4L	7.98E-005	0.020604536	1.137377	2.199807032
BC002984	THTPA	8.01E-005	0.020604536	0.619879	1.536746559
BC101631	CYP3A4	8.13E-005	0.020798939	1.773076	3.41781858
NM_018244	C20orf44	8.24E-005	0.020971002	0.781028	1.718354723
NM_152277	DC-UbP	8.34E-005	0.021096576	-0.53018	-1.444110612

Continued

NM_139005	HFE	8.51E-005	0.021123479	0.466799	1.382040016
CR594512	FDXR	8.52E-005	0.021123479	1.944309	3.848535056
AF092844	MDM2	8.56E-005	0.021123479	1.246143	2.372064052
NM_000514	GDNF	8.57E-005	0.021123479	1.841456	3.583714249
XM_926697	FLJ44451	8.63E-005	0.021123479	0.665459	1.586072686
NM_001024938	SLC2A11	8.65E-005	0.021123479	0.691689	1.615173505
NM_018161	NADSYN1	8.68E-005	0.021123479	0.965844	1.95320651
NM_022497	MRPS25	8.77E-005	0.021214728	0.39213	1.312329298
NM_194430	RNASE4	8.85E-005	0.021214728	-0.32499	-1.252658661
NM_152718	VWCE	8.86E-005	0.021214728	3.125943	8.729768798
BX647267	HMGB1	9.07E-005	0.021395376	-0.64022	-1.558566661
BC106879	STRN	9.07E-005	0.021395376	-0.58613	-1.501215357
AM180330	BLNK	9.07E-005	0.021395376	2.739121	6.676633227
BC011735	PLSCR3	9.22E-005	0.021617615	0.600885	1.51664708
NM_006404	PROCR	9.34E-005	0.021803886	0.99811	1.997381787
NM_018275	FLJ10925	9.54E-005	0.021836594	0.768826	1.703882289
XM_928682	LOC645671	9.54E-005	0.021836594	-0.55613	-1.470318841
NM_024531	GPR172A	9.54E-005	0.021836594	0.448516	1.364635899
NM_032601	MCEE	9.55E-005	0.021836594	1.075926	2.108075068
BC005359	GMFB	9.74E-005	0.022004015	-0.35951	-1.282988834
NM_032038	SPIN1	9.81E-005	0.022004015	0.467335	1.382552939
BC035817	FLJ11286	9.83E-005	0.022004015	0.8416	1.792036255
NM_175063	LOC284361	9.97E-005	0.022004015	0.569923	1.48444383
NM_003146	SSRP1	1.00E-004	0.022004015	-0.34641	-1.271390356
NM_000794	DRD1	0.000100151	0.022004015	1.297878	2.45866995
AF258573	RBED1	0.00010043	0.022004015	0.779479	1.71651036
NM_002673	PLXNB1	0.000100515	0.022004015	1.068407	2.097116451
NM_019103	ZMAT5	0.000100656	0.022004015	0.816691	1.761361448
BC002869	STXBP2	0.000101753	0.022136538	0.848131	1.800166728
BC013294	DKFZP564O0823	0.000102563	0.022205475	1.195626	2.290441291
XM_929677	LOC286239	0.000103721	0.022348661	-0.83317	-1.781593484
NM_001120	TETTRAN	0.000105315	0.022584127	0.62249	1.539529861
NM_005749	TOB1	0.000106266	0.022679932	0.435847	1.352704688
NM_002917	RFNG	0.000107727	0.022797458	0.497059	1.411333856
XM_375806	DENND4B	0.000108328	0.022797458	0.446105	1.362357412
BC053675	TMPO	0.000108513	0.022797458	-1.69503	-3.237831441

Continued

NM_003562	SLC25A11	0.000109199	0.022797458	0.490737	1.405162277
NM_013314	BLNK	0.000109348	0.022797458	2.921617	7.576950496
AK097937	unknown	0.000110195	0.022868298	-0.55121	-1.465310533
NM_001127	AP1B1	0.000111364	0.022991949	0.789246	1.728171284
NM_016462	TMEM14C	0.000111812	0.022991949	0.299215	1.230474297
NM_182543	NSUN6	0.000112462	0.023020471	0.500217	1.414426187
NM_030648	SETD7	0.000113028	0.02303167	-0.28057	-1.214671718
NM_198044	ZDHHC16	0.000114044	0.023082388	0.320138	1.248449664
NM_001657	AREG	0.000114302	0.023082388	1.416703	2.669747068
U46461	DVL1	0.000115408	0.023139525	0.403262	1.32249436
AK055216	QTRT1	0.000116011	0.023139525	0.664524	1.585045621
X53280	BTF3	0.00011642	0.023139525	0.36662	1.289328687
NM_014855	KIAA0415	0.000116641	0.023139525	0.754598	1.687161907
AX775899	unknown	0.000117789	0.023231215	0.567198	1.481643398
BC104982	IL12A	0.000118293	0.023231215	1.159623	2.233990988
NM_000422	KRT17	0.00011865	0.023231215	-0.69737	-1.621551574
AK055636	ANTXR2	0.000120044	0.023283202	-0.39239	-1.312570321
BC033907	SHC4	0.000120661	0.023283202	1.848102	3.600262955
NM_024112	C9orf16	0.000120759	0.023283202	0.585317	1.500368858
BC058160	LOC554234	0.000120984	0.023283202	-1.00962	-2.013380045
AK097538	FLJ21736	0.000121598	0.023301705	2.698498	6.491259401
XM_933562	LOC643556	0.000122153	0.023308956	0.452226	1.368149336
NM_013274	POLL	0.000124176	0.02345206	0.582656	1.497603411
NM_001009925	C20orf30	0.000124452	0.02345206	0.354268	1.278336452
NM_175841	SMO	0.000124695	0.02345206	0.776625	1.713118955
NM_014014	ASCC3L1	0.00012594	0.02345206	0.486793	1.401326211
NM_014267	C11orf58	0.000125968	0.02345206	-0.23582	-1.177577381
NM_015133	MAPK8IP3	0.000126515	0.02345206	0.541048	1.455028988
NM_003858	CCNK	0.000126699	0.02345206	0.259691	1.197222071
NM_022372	GBL	0.000127327	0.02345206	0.384275	1.305203284
NM_015949	C7orf20	0.00012759	0.02345206	0.719948	1.647123179
NM_003946	NOL3	0.000128894	0.02352597	0.763178	1.697224864
BC012362	RAP2B	0.000129037	0.02352597	0.843525	1.7944289
NM_006396	SSSCA1	0.000130792	0.023749891	0.581673	1.496583596
BC047881	FAM8A1	0.000134324	0.024293183	-0.63622	-1.554255431
BC022276	CPM	0.000135709	0.024319547	1.734674	3.328041804

Continued

NM_012075	C16orf35	0.000136684	0.024319547	0.634592	1.552498833
NM_024927	PLEKHH3	0.000137188	0.024319547	0.96858	1.956912925
NM_005834	TIMM17B	0.000137441	0.024319547	0.709074	1.634754262
NM_015679	TRUB2	0.000137511	0.024319547	0.50177	1.415949904
BC065235	SPIN1	0.000137864	0.024319547	0.330978	1.257866109
NM_207329	MYADML	0.00013825	0.024319547	-0.40323	-1.322464391
NM_017865	ZNF692	0.000140582	0.02463352	0.890252	1.853499829
BC013116	CLIPR-59	0.000143743	0.025038337	0.458221	1.373846884
NM_031957	KRTAP1-5	0.00014464	0.025038337	1.160349	2.235115291
NM_004148	NINJ1	0.00014472	0.025038337	0.928226	1.902933983
NM_024741	ZNF408	0.000145116	0.025038337	0.606996	1.523084531
XM_933610	LOC643556	0.000150267	0.025631098	0.78141	1.718810229
NM_032326	MGC4618	0.000150727	0.025631098	0.52004	1.433994804
NM_022749	RAI16	0.000151485	0.025631098	0.702885	1.627756994
BC112920	HSPA8	0.000151565	0.025631098	-0.23666	-1.178260308
NM_001002843	SUHW4	0.000152012	0.025631098	-0.24981	-1.189051217
BC006567	SYMPK	0.000152346	0.025631098	0.341263	1.266864828
NM_005526	HSF1	0.000152536	0.025631098	0.536363	1.450311334
NM_001009812	LBX2	0.000155647	0.026056749	0.562814	1.477147166
NM_004864	GDF15	0.000157544	0.026242679	1.928	3.805272285
NM_024661	CCDC51	0.000159507	0.026242679	1.098491	2.141306089
NM_175840	SMO	0.000159737	0.026242679	0.643258	1.561851966
XM_930679	RP11-144G6.7	0.000160465	0.026242679	0.61926	1.536087253
BC000653	DNPEP	0.000160559	0.026242679	0.274029	1.209180082
NM_004377	CPT1B	0.000161008	0.026242679	1.008058	2.011202224
NM_177938	PH-4	0.000161173	0.026242679	0.523886	1.437823097
NM_002337	LRPAP1	0.00016142	0.026242679	0.642737	1.561288503
AF201370	MDM2	0.000162009	0.026243671	1.242205	2.365597313
BC112054	VARSL	0.000163921	0.026401856	0.476734	1.391590266
NM_080593	HIST1H2BK	0.000164158	0.026401856	1.408705	2.654987956
AK092491	unknown	0.000165057	0.026451984	0.591021	1.506312004
BC069757	PRO1768	0.000165746	0.026468295	0.903213	1.870227053
NM_004073	PLK3	0.000167437	0.026643797	1.019965	2.027869531
NM_001033053	NALP1	0.000169306	0.026846387	0.795635	1.735840854
NM_016535	ZNF581	0.000170936	0.026945444	0.339112	1.264977525
NM_181493	ITPA	0.000171744	0.026945444	0.530141	1.444070164

Continued

AK056120	CCNL2	0.00017175	0.026945444	0.621656	1.538639833
XM_211367	LOC284184	0.000172581	0.026945444	1.006507	2.009040442
NM_001146	ANGPT1	0.000172923	0.026945444	-0.48271	-1.39736319
NM_031232	NECAB3	0.000175342	0.027228157	0.974428	1.964862444
NM_032621	BEX2	0.000176565	0.027323873	0.913273	1.883313264
BC002359	TSN	0.000177905	0.027436973	-0.17092	-1.125773416
BC032244	REXO1	0.000179497	0.027445671	0.588425	1.503604011
NM_175047	PILRB	0.000179534	0.027445671	0.586563	1.501664658
BC070035	NR1D2	0.000179839	0.027445671	-0.65656	-1.576323788
NM_016826	OGG1	0.000180399	0.027445671	0.509329	1.423387779
NM_001004426	PLA2G6	0.000182006	0.027493944	1.292141	2.448912101
NM_001376	DYNC1H1	0.000182718	0.027493944	0.579959	1.494806357
NM_198850	PHLDB3	0.000183038	0.027493944	1.312085	2.483000613
BC035214	SRPK2	0.00018384	0.027493944	-0.33381	-1.260334799
NM_001010915	PTPLAD2	0.000184367	0.027493944	-0.70564	-1.630870668
NM_001001824	OR2T27	0.000185297	0.027493944	-0.50226	-1.416426308
BC063785	PGBD2	0.000185833	0.027493944	0.789353	1.728298857
NM_018467	MDS032	0.000186501	0.027493944	0.423527	1.341202599
NM_031472	TRPT1	0.000187663	0.027493944	0.836842	1.786135753
AJ278977	MDM2	0.000188358	0.027493944	1.583683	2.997339642
AK000938	ZNF691	0.000188929	0.027493944	0.51907	1.433031363
NM_004567	PFKFB4	0.00018918	0.027493944	1.213481	2.318964224
NM_004699	FAM50A	0.000189284	0.027493944	0.560794	1.475080667
NM_003522	HIST1H2BF	0.000189863	0.027493944	0.761616	1.695388163
BC031077	GRIN2C	0.000189874	0.027493944	1.273981	2.418278908
BC064570	C11orf31	0.000191739	0.027583135	0.677328	1.599174971
NM_153335	LYK5	0.000192279	0.027583135	0.666599	1.587326787
NM_147184	TP53I3	0.000192629	0.027583135	1.059109	2.083644115
BC038094	IFT20	0.000194391	0.027583135	0.413852	1.332237719
NM_145036	CCDC46	0.000194889	0.027583135	-0.70213	-1.626904814
NM_000254	MTR	0.000195442	0.027583135	-0.20971	-1.156458238
NM_001033551	TOM1L2	0.000195803	0.027583135	0.53162	1.445551101
BC069119	GDNF	0.000197027	0.027583135	1.773429	3.418655826
AK127093	DGKA	0.000197158	0.027583135	1.105381	2.151557067
NM_198061	CES2	0.000197303	0.027583135	0.917607	1.888979962
BC069753	RFPL3	0.000197628	0.027583135	0.796727	1.737155061

Continued

BC065741	RPUSD3	0.000197841	0.027583135	0.719335	1.646423204
NM_207013	TCEB2	0.000199815	0.027772422	0.41621	1.334417611
NM_005343	HRAS	0.000202496	0.02805564	0.952672	1.935454573
AL136869	RECQL5	0.000203389	0.02805564	0.788046	1.726734645
NM_024417	FDXR	0.000203722	0.02805564	1.976774	3.936118473
BC001573	LOC134147	0.000204697	0.028104091	0.62485	1.542051006
NM_006693	CPSF4	0.000205537	0.028133633	0.753082	1.685388912
NM_030974	SHARPIN	0.000206902	0.028234534	0.542625	1.456620032
BC008962	GDF15	0.000209322	0.028330161	1.922825	3.791647032
AK090418	LOC349196	0.000209381	0.028330161	-0.68897	-1.612130327
XM_933916	GPR108	0.00020949	0.028330161	0.412805	1.331271862
AK123115	NAT9	0.000211405	0.028405248	0.62965	1.547189857
BC000417	SMUG1	0.000213217	0.028405248	0.668187	1.589074761
NM_001039492	FHL2	0.00021421	0.028405248	0.773943	1.709936952
AK223604	CYFIP2	0.000214732	0.028405248	3.177553	9.047709169
NM_022772	EPS8L2	0.000214836	0.028405248	1.154149	2.225530768
NM_006899	IDH3B	0.000214892	0.028405248	0.504906	1.419030684
BC029796	LOC116349	0.000215027	0.028405248	1.14759	2.215434966
NM_005824	LRRC17	0.000215091	0.028405248	-0.39195	-1.312168817
BC106720	HIST1H2BO	0.000216316	0.028483475	0.693951	1.617708004
NM_016448	DTL	0.000217429	0.028546628	-2.31246	-4.967286515
NM_001283	AP1S1	0.000219159	0.02859037	0.736157	1.665732546
NM_004060	CCNG1	0.000219566	0.02859037	0.241311	1.182066624
NM_005704	PTPRU	0.000220214	0.02859037	0.825715	1.772413442
CR610028	ZDHHC16	0.000220302	0.02859037	0.325452	1.253056768
NM_022156	DUS1L	0.000222748	0.0286294	0.460923	1.37642211
NM_014186	COMMD9	0.000223284	0.0286294	0.628971	1.546461825
NM_152464	C17orf32	0.000223518	0.0286294	0.55106	1.465162034
AB102799	unknown	0.000223675	0.0286294	-0.38602	-1.306780982
NM_014226	RAGE	0.000223781	0.0286294	0.706431	1.631762309
NM_000765	CYP3A7	0.000225072	0.028712956	1.666446	3.174316309
NM_001039675	UNC45A	0.000227659	0.028960937	0.381496	1.302692019
BC029882	CART	0.000228537	0.028990748	-0.47724	-1.392077141
NM_000481	AMT	0.000230169	0.029023322	0.548327	1.462389039
NM_004881	TP53I3	0.000230946	0.029023322	1.106592	2.153364416
XM_929276	LOC646342	0.000232092	0.029023322	-1.34154	-2.534214705

Continued

U33203	MDM2	0.000232208	0.029023322	1.171052	2.251758686
NM_001035506	FLJ21839	0.000232426	0.029023322	0.556005	1.470192554
NM_201556	FHL2	0.000232661	0.029023322	0.652791	1.572206545
NM_001834	CLTB	0.000234853	0.029159542	0.313156	1.242422257
NM_005319	HIST1H1C	0.000235422	0.029159542	1.225939	2.339076533
BC050345	SEPT10	0.000235835	0.029159542	-0.41262	-1.331102002
BC105791	C20orf44	0.000236908	0.029159542	0.754831	1.68743381
BC000154	SLC12A9	0.000237272	0.029159542	0.543844	1.45785213
NM_004809	STOML1	0.000237638	0.029159542	0.616827	1.53349915
NM_030816	ANKRD13C	0.000239066	0.029255075	-0.60548	-1.52148541
NM_022116	FIGNL1	0.000244442	0.02983187	-0.79284	-1.732480111
BC036742	PLA2G6	0.000250372	0.030472932	1.108781	2.156633383
BC006152	ASPSCR1	0.000251285	0.030501655	0.349574	1.274183987
NM_018838	NDUFA12	0.000254539	0.030770071	0.218751	1.163725942
NM_006306	SMC1L1	0.000255217	0.030770071	-0.66316	-1.583550165
NM_145183	PYCARD	0.000256379	0.030770071	0.533324	1.447260005
BC035576	MAP3K14	0.000256524	0.030770071	0.491708	1.406108487
NM_030751	ZEB1	0.000256913	0.030770071	-0.45281	-1.368707647
NM_207344	SPRYD4	0.000258127	0.030833545	0.524439	1.438373851
NM_001013841	STAP2	0.000262317	0.03120059	0.321729	1.249827263
NM_017495	RNPC1	0.000262586	0.03120059	0.733735	1.662938373
NM_024623	OGFOD2	0.000263909	0.031275326	0.745877	1.676993137
AB037861	INTS1	0.000266398	0.031375578	0.444582	1.360919653
NM_006591	POLD3	0.000266734	0.031375578	-0.57512	-1.489796667
BC032095	CES2	0.000266845	0.031375578	0.790558	1.729742948
NM_203437	AFTIPHILIN	0.000270841	0.031762474	0.800571	1.741790599
NM_005611	RBL2	0.000273561	0.031998156	-0.63408	-1.551943397
NM_012423	RPL13A	0.000274644	0.032041546	0.216508	1.161917881
AK090774	PLCD1	0.000278061	0.03229583	0.814386	1.758550007
NM_014853	RUTBC1	0.000278258	0.03229583	0.620561	1.537472941
CR595121	ZNF692	0.000279733	0.032340087	0.670359	1.591469142
CR606194	unknown	0.000280488	0.032340087	0.707067	1.632481836
BC093622	BLM	0.000280794	0.032340087	-2.38397	-5.219694079
NM_012135	FAM50B	0.000283927	0.032602086	-0.59321	-1.508594915
BC041692	ACSL3	0.000284786	0.032602086	-0.61671	-1.533372395
BC067898	ZDHHC20	0.00028524	0.032602086	-0.58069	-1.49556317

Continued

NM_004125	LOC552891	0.000287751	0.032663206	0.569796	1.484313935
NM_058004	PIK4CA	0.000288373	0.032663206	0.581922	1.496842174
AK127235	FLYWCH1	0.000288393	0.032663206	0.549769	1.463850874
BC066553	C6orf114	0.000288676	0.032663206	-0.39632	-1.316145963
BC080636	EPS8L2	0.000291314	0.032801406	1.15071	2.220231173
NM_199234	GDNF	0.000291705	0.032801406	2.336181	5.049642771
NM_173161	IL1F10	0.000292083	0.032801406	0.342449	1.267906873
NM_000107	DDB2	0.000292954	0.032817448	1.361112	2.568831693
NM_003969	UBE2M	0.000295824	0.033056648	0.214702	1.160464083
NM_014956	CEP164	0.000300126	0.033446965	0.766103	1.700669186
AY358250	SHC4	0.000300911	0.033446965	1.537039	2.901982678
NM_001037633	SIL1	0.00030182	0.033446965	0.510697	1.424737934
AF289556	unknown	0.000302288	0.033446965	-0.4752	-1.390107465
NM_016821	OGG1	0.000306048	0.033717588	1.116248	2.16782479
NM_017750	RetSat	0.00030691	0.033717588	0.585687	1.500753354
NM_001037332	CYFIP2	0.00030698	0.033717588	2.244177	4.737668883
NM_001005920	LOC339123	0.000309198	0.033833427	0.369975	1.292330793
XM_932685	LOC653257	0.000309537	0.033833427	1.254491	2.385830228
NM_005101	ISG15	0.000311192	0.033931982	0.528482	1.442410374
BC000902	LOC51035	0.000312751	0.034019647	0.453639	1.369489851
AB000409	MKNK1	0.000314983	0.03417983	0.468028	1.3832179
NM_002555	SLC22A18	0.000316186	0.034227854	0.655054	1.574674833
XM_378223	RP11-144G6.7	0.000319826	0.03448507	0.692693	1.616297445
NM_017547	FOXRED1	0.000320093	0.03448507	0.958495	1.943282204
NM_001008658	TUBGCP6	0.000321983	0.034605824	0.787161	1.72567557
NM_032867	MICALCL	0.000322788	0.034609766	0.834278	1.782964584
BC004225	NAT9	0.000325171	0.034782474	0.478233	1.393036858
NM_005262	GFER	0.000327341	0.034931651	0.642039	1.560533448
NM_006221	PIN1	0.000329519	0.035011877	0.459173	1.374753776
NM_007188	ABCB8	0.000330308	0.035011877	0.854056	1.807575422
BC100808	SLC2A11	0.000332004	0.035011877	1.12017	2.173725869
NM_024028	MGC3265	0.000332425	0.035011877	0.776621	1.713113982
NM_145804	ABTB2	0.000332811	0.035011877	1.178724	2.263764586
NM_001054	SULT1A2	0.000333139	0.035011877	0.4522	1.368125328
NM_020246	SLC12A9	0.000333654	0.035011877	0.691581	1.615052801
BC011895	COQ4	0.000334313	0.035011877	0.873778	1.832455715

Continued

XM_928494	LOC645463	0.000337968	0.035243929	-0.6093	-1.525516392
AK000346	NFYC	0.000338128	0.035243929	0.395006	1.314948582
BC000995	SFN	0.000338876	0.035243929	1.133907	2.194522783
NM_007245	ATXN2L	0.000341202	0.035404018	0.44118	1.35771461
NM_015654	NAT9	0.000343057	0.035425893	0.653522	1.573003434
M97190	SP2	0.000343098	0.035425893	0.421224	1.339063212
NM_019099	C1orf183	0.000343773	0.035425893	1.859789	3.629546054
NM_176826	ILVBL	0.000346356	0.035593942	0.638558	1.556771878
AK002100	PHCA	0.000346984	0.035593942	-0.67345	-1.594886159
NM_206538	LOC284361	0.000348836	0.035610637	0.677604	1.599480637
XM_926234	LOC642832	0.000349136	0.035610637	2.801435	6.971336226
NM_005224	ARID3A	0.000349573	0.035610637	0.738044	1.667912826
BC017296	SESN3	0.00035043	0.035610637	-0.64667	-1.565545927
NM_183010	TNRC5	0.000351314	0.035610637	0.557644	1.471863928
BC112240	NEK8	0.000351892	0.035610637	0.755989	1.68878919
NM_005028	PIP5K2A	0.000353302	0.035673222	-0.51575	-1.429738976
NM_019057	FLJ10404	0.000354735	0.035737732	0.299024	1.230311471
BC067895	unknown	0.000356722	0.035827149	0.760347	1.693897859
BC037542	MIB2	0.000357213	0.035827149	1.042387	2.059632378
AF318352	SCRIB	0.000360145	0.036040916	1.322689	2.501318626
AK131264	ZNF184	0.000361971	0.036143343	-0.42906	-1.346358283
NM_005072	SLC12A4	0.000364395	0.036304905	0.587911	1.503068511
BC016480	PPM1D	0.000365857	0.036370105	0.663197	1.583587673
NM_001098	ACO2	0.000367039	0.036407216	0.582543	1.497486847
BC002355	HNRNPA1	0.000369897	0.03661	-0.40463	-1.323747314
NM_030807	SLC2A11	0.000373583	0.036893753	0.790317	1.72945384
NM_002624	PFDN5	0.000375613	0.037013106	0.454234	1.370055507
NM_015106	RAD54L2	0.000378885	0.037046217	0.529344	1.443273233
BC005402	UCRC	0.000379806	0.037046217	0.407152	1.326065024
BC020586	SFRS14	0.000381952	0.037046217	0.382491	1.303591177
NM_181775	PLXNA4B	0.000382734	0.037046217	-0.91692	-1.888078766
NM_145752	CDIPT	0.00038475	0.037046217	0.213113	1.159186657
BC008041	CPSF3L	0.000384919	0.037046217	0.78296	1.720657928
BC074737	NEURL2	0.000384938	0.037046217	0.869833	1.827451531
NM_001735	C5	0.000385212	0.037046217	-0.54227	-1.456259309
BC112036	SESN1	0.000385582	0.037046217	0.927843	1.902430011

Continued

BC112271	KIF7	0.000386563	0.037046217	0.423367	1.341053551
NM_004705	PRKRIR	0.000387168	0.037046217	-0.43051	-1.347713676
NM_005811	GDF11	0.000387397	0.037046217	0.491275	1.405686494
BC006821	CBX5	0.000387718	0.037046217	-0.8314	-1.779408002
NM_018518	MCM10	0.000387731	0.037046217	-1.11931	-2.172436272
BC072681	ZA20D1	0.00038849	0.037046217	-0.37656	-1.298244539
NM_172208	TAPBP	0.000389112	0.037046217	0.371858	1.294018284
BC016965	NALP1	0.000391298	0.037175754	0.622137	1.539153399
AF119833	PFTK1	0.000393602	0.037315912	-0.61391	-1.530403638
BC029832	ZYG11B	0.000394649	0.037336601	-0.40264	-1.321925631
BC006085	ARFGAP1	0.000395657	0.03735347	0.501176	1.415366932
NM_006828	ASCC3	0.000399476	0.03759174	0.762191	1.696064548
NM_003523	HIST1H2BE	0.00039985	0.03759174	0.694035	1.617802154
NM_014595	NT5C	0.000401455	0.037629454	0.406239	1.325226624
XM_932195	LOC643009	0.000401922	0.037629454	1.417885	2.671935638
NM_005708	GPC6	0.00040296	0.037648318	-0.54018	-1.454152886
NM_032307	C9orf64	0.000405457	0.037803195	-0.48593	-1.400492657
XM_932681	LOC653257	0.000410478	0.038192227	1.154277	2.225727344
NM_005275	GNL1	0.00041168	0.038225153	0.339328	1.265167058
NM_003422	MZF1	0.00041395	0.038280175	0.625641	1.542895806
CR603836	NECAB3	0.000413973	0.038280175	0.848887	1.801111148
NM_006528	TFPI2	0.000415782	0.038317879	0.538901	1.452865079
NM_148936	NSUN5C	0.000416082	0.038317879	0.66244	1.582757005
NM_002488	NDUFA2	0.000420786	0.038671971	0.66155	1.581781201
AK127078	unknown	0.000421693	0.038676392	0.457317	1.372985729
NM_138761	BAX	0.000423442	0.038757835	0.671702	1.59295118
BC066952	NEFL	0.000425486	0.038817021	1.196854	2.292391985
BC022483	ARHGAP29	0.000426312	0.038817021	-0.58768	-1.502825756
BC026066	ASCC3	0.000429227	0.038817021	0.370185	1.29251859
NM_138644	CABYR	0.000429394	0.038817021	0.529255	1.443183614
NM_015382	HECTD1	0.000429588	0.038817021	-0.1033	-1.074230028
NM_080916	DGUOK	0.000430517	0.038817021	0.479929	1.394674573
BC017379	HIST1H2AC	0.000431396	0.038817021	0.943462	1.923137625
NM_022064	RNF123	0.000431692	0.038817021	0.643427	1.562035439
BC047118	MGC13114	0.000431846	0.038817021	0.682263	1.604654629
CR612107	TUSC4	0.000434127	0.038944317	0.624511	1.541688603

Continued

NM_019884	GSK3A	0.000435021	0.038946913	0.394097	1.31411962
NM_014922	NALP1	0.000441654	0.039462292	0.629958	1.547519526
NM_001010883	FAM102B	0.000443307	0.039467272	-0.53097	-1.444896798
AF258572	GSDML	0.000443846	0.039467272	0.500293	1.414500324
XM_929819	LOC646861	0.000444822	0.039467272	-1.05102	-2.071991092
NM_203288	RP9	0.000445215	0.039467272	0.4274	1.344807868
AK125455	ZNF337	0.000446625	0.039504248	0.739711	1.669840787
NM_014699	ZNF646	0.0004476	0.039504248	0.629384	1.546904698
NM_030645	SH3BP5L	0.000448264	0.039504248	0.754456	1.686995688
NM_004581	RABGGTA	0.000451259	0.039690493	0.810738	1.75410845
BC074979	DRD1	0.000452229	0.039698293	1.306172	2.472844797
NM_002719	PPP2R5C	0.00045425	0.039798096	-0.46495	-1.380270296
AK074112	CCNL2	0.000461899	0.040382561	0.523248	1.437187635
NM_001003689	L3MBTL2	0.000462714	0.040382561	0.704667	1.629768084
NM_005273	GNB2	0.000464199	0.04039402	0.54869	1.462756695
XM_933425	LOC653319	0.000464639	0.04039402	0.549828	1.463910651
AK126163	ARHGAP30	0.000470269	0.040779788	0.95674	1.940919473
NM_001191	BCL2L1	0.000471659	0.040779788	1.236457	2.356191072
NM_181745	GPR120	0.000471793	0.040779788	-0.56003	-1.474302679
NM_031209	QTRT1	0.000474274	0.040885399	0.526729	1.440659555
NM_003717	NPFF	0.000474831	0.040885399	0.756762	1.689694021
NM_019001	XRN1	0.000476599	0.040959305	-0.33327	-1.259867696
NM_001002245	ANAPC11	0.000478765	0.041027328	0.622674	1.539726645
BC037236	DUSP6	0.000479212	0.041027328	0.550383	1.464474844
NM_133175	APBB3	0.000480821	0.041086888	0.870727	1.828584152
NM_001037811	HSD17B10	0.000484076	0.041228893	0.310014	1.239720113
BC008692	PTPN11	0.000484883	0.041228893	-0.33927	-1.265112308
NM_006340	BAIAP2	0.000485229	0.041228893	0.364064	1.287045913
NM_020317	C1orf63	0.000488178	0.041343077	0.783606	1.721428019
NM_032878	ALKBH6	0.000488753	0.041343077	0.779517	1.716556482
NM_001005845	ADAM9	0.000490126	0.041343077	-0.60635	-1.52240188
BC082977	unknown	0.000490245	0.041343077	1.373963	2.591816326
BC044216	BAG5	0.000491284	0.041353283	-0.40791	-1.326764266
AK074137	CCDC95	0.000496135	0.04168363	0.602465	1.518308114
NM_001014837	CUTA	0.000498128	0.041773213	0.530065	1.443994594
BC098342	CSAD	0.00051218	0.0428148	0.593121	1.508506922

Continued

AB051543	SYNE1	0.000515072	0.0428148	1.896385	3.722791433
NM_013347	RPA4	0.000515409	0.0428148	0.847504	1.799385386
AK055835	OSBPL8	0.000516434	0.0428148	-0.416	-1.334226164
NM_032204	ASCC2	0.000517193	0.0428148	0.414808	1.333120959
NM_013961	NRG1	0.000518384	0.0428148	2.575704	5.961618096
NM_003427	ZNF76	0.000519132	0.0428148	0.721459	1.648848457
XM_290777	ARL16	0.00051956	0.0428148	0.36928	1.291708172
BC035152	unknown	0.000519799	0.0428148	0.718988	1.64602749
BC014165	GLI4	0.000520862	0.0428148	1.079039	2.112628722
NM_005044	PRKX	0.000521007	0.0428148	0.579234	1.494055797
NM_145316	C6orf128	0.000522289	0.042841971	1.728398	3.313595802
BC045712	GPC1	0.00053116	0.043463852	0.92762	1.902135661
NM_022091	ASCC3	0.000531801	0.043463852	0.644132	1.562799235
BC037283	ZMPSTE24	0.000536121	0.043713469	-0.58085	-1.495729639
BC011968	DECR2	0.000536796	0.043713469	0.958622	1.943452159
NM_152619	DCAMKL2	0.00054278	0.04405283	-0.4426	-1.359048233
BC067819	TMEM29	0.00054292	0.04405283	0.626882	1.544223621
AK057461	C22orf25	0.000549901	0.044539022	0.49342	1.407778411
NM_181690	AKT3	0.000555888	0.044943089	-0.39999	-1.319496263
BC036557	KIAA1394	0.000557531	0.044958077	1.200662	2.298450457
BC011250	MTMR1	0.00055807	0.044958077	0.406178	1.325170515
BC071709	ERH	0.00056312	0.045087179	-0.2315	-1.174054907
NM_005176	ATP5G2	0.000564545	0.045087179	0.633518	1.551343512
BC101727	MCM10	0.000567888	0.045087179	-3.05493	-8.310486809
NM_001013845	CXorf40B	0.000568212	0.045087179	0.435675	1.352543365
NM_007108	TCEB2	0.000568367	0.045087179	0.485256	1.39983404
CR607247	DDOST	0.000568746	0.045087179	0.213825	1.159759031
NM_017575	SMG6	0.000568925	0.045087179	0.464246	1.37959624
AF172850	LOC51152	0.000569645	0.045087179	0.689944	1.613220628
BC090039	C1orf160	0.000571448	0.045087179	0.693795	1.617533221
NM_015421	C16orf51	0.000571623	0.045087179	0.659743	1.57980083
XM_292717	DKFZp779B1634	0.000573525	0.045087179	-0.89427	-1.858667629
NM_152355	ZNF441	0.00057355	0.045087179	0.884635	1.846297236
BC014428	MTRF1L	0.000573717	0.045087179	0.291276	1.223722182
NM_153268	PLCXD2	0.000573916	0.045087179	1.089582	2.128124016
BC009932	GLTP	0.000574691	0.045087179	0.713061	1.639278722

Continued

NM_003876	TMEM11	0.000578803	0.04532703	0.579878	1.494722798
BC021229	SELI	0.000579761	0.04532703	-0.41266	-1.331135809
NM_153763	KCNC4	0.000581221	0.045342305	1.10146	2.145717145
BC041887	unknown	0.00058197	0.045342305	0.566878	1.481314735
AK097425	ACAD10	0.000585666	0.045551433	0.516721	1.430699479
NM_032344	NUDT22	0.000591831	0.045806523	0.353802	1.277923772
NM_006322	TUBGCP3	0.000592095	0.045806523	-0.35559	-1.27950511
NM_152640	DCP1B	0.000592794	0.045806523	0.772194	1.70786523
BC052993	FAM53C	0.000593014	0.045806523	-0.33894	-1.264823925
BC062330	XX-FW81657B9.4	0.000594205	0.045817509	0.939121	1.91735985
NM_178336	MRPL52	0.000595191	0.045817509	0.518488	1.432453574
BC032466	NAPRT1	0.00059663	0.045849872	0.929263	1.904302534
CR605903	NSFL1C	0.000601294	0.046129631	0.60684	1.52291939
NM_014727	MLL2	0.000602344	0.046131591	0.524873	1.438806547
NM_006835	CYC1	0.000605633	0.046304705	-0.42322	-1.340916298
BC002697	PPP1CB	0.00060952	0.046452014	-0.45464	-1.370436438
AK023219	PBXIP1	0.000610331	0.046452014	0.221299	1.165783092
XM_929117	LOC392232	0.000610654	0.046452014	-2.12231	-4.353895338
NM_004259	RECQL5	0.000613323	0.046528137	0.856715	1.810910077
XM_928224	LOC653583	0.000616444	0.046528137	1.623175	3.080522425
NM_020155	GPR137	0.000617221	0.046528137	0.615799	1.532406487
BC000637	DHRS7	0.000617844	0.046528137	0.476058	1.390938127
AF068181	BLNK	0.000619257	0.046528137	2.422056	5.359342771
XM_932091	CEP78	0.000619624	0.046528137	-0.81447	-1.758649574
NM_004099	STOM	0.000619923	0.046528137	0.884093	1.845603629
NM_001618	PARP1	0.000622183	0.046528137	-0.31139	-1.240902535
NM_017421	COQ3	0.000622434	0.046528137	0.378414	1.299911897
NM_025072	PTGES2	0.000622467	0.046528137	0.402225	1.321544306
NM_000920	PC	0.00062302	0.046528137	0.562699	1.477030351
AK124869	SH2D5	0.000624509	0.046562126	0.577474	1.492234623
NM_053052	C1orf142	0.000626004	0.046596443	0.512315	1.426337189
XM_930966	LOC642637	0.000628024	0.046604738	0.923966	1.897324111
NM_001001551	C9orf103	0.000629529	0.046604738	0.459762	1.375315134
NM_018309	TBC1D23	0.000629772	0.046604738	-0.23405	-1.17613531
NM_014891	PDAP1	0.000630255	0.046604738	0.368011	1.290572433
NM_001008393	LOC201725	0.000635187	0.046892446	-1.0742	-2.105558118

Continued

NM_022374	ARL6IP2	0.000637328	0.046910385	-0.41289	-1.331350194
NM_013362	ZNF225	0.000637514	0.046910385	-0.51455	-1.428547369
NM_033415	ARMC6	0.000643082	0.047187228	0.579687	1.494525122
NM_001012706	LOC283551	0.000644706	0.047187228	0.373978	1.295921129
XM_930936	unknown	0.000645181	0.047187228	-0.24036	-1.181290415
NM_001005909	IHPK2	0.000645467	0.047187228	0.751259	1.683260629
BC093739	AP3B2	0.00064894	0.047244081	1.555147	2.93863623
NM_005094	SLC27A4	0.000650072	0.047244081	0.730493	1.659206337
XM_497141	LOC441511	0.000650431	0.047244081	-0.36004	-1.283461958
NM_000757	CSF1	0.000650441	0.047244081	0.73629	1.665886383
NM_005143	HP	0.000653102	0.047360936	0.690281	1.613597539
BC058843	ZBTB8OS	0.000656165	0.047365676	0.365143	1.288008949
NM_006779	CDC42EP2	0.000656681	0.047365676	1.124931	2.180911386
NM_152436	MGC39497	0.000656822	0.047365676	0.388693	1.309206347
AK025630	RBED1	0.000657375	0.047365676	0.595552	1.51105023
BC052639	MRPL43	0.000660028	0.047381968	0.387599	1.308214787
NM_001029874	REP15	0.000661069	0.047381968	0.622925	1.539993892
NM_014947	FOXJ3	0.000661342	0.047381968	-0.25004	-1.189241904
NM_001010887	ASAH3L	0.000664726	0.047381968	1.260625	2.395994965
BC070096	C3orf63	0.000665405	0.047381968	-0.49131	-1.405725312
BC005338	CAPZA2	0.000665851	0.047381968	-0.32785	-1.255142019
NM_015997	C1orf66	0.000666251	0.047381968	0.781647	1.719092538
NM_033419	PERLD1	0.000666887	0.047381968	0.771842	1.707448677
NM_020680	SCYL1	0.000667862	0.047381968	0.335349	1.261682792
NM_024945	C9orf76	0.000668122	0.047381968	-0.41692	-1.335071268
NM_031450	C11orf68	0.000669492	0.047404423	0.461952	1.3774046
BC040516	SGIP1	0.000671645	0.04747299	0.782768	1.720428854
AK125726	unknown	0.000672894	0.04747299	0.798684	1.739513851
BC020690	LY96	0.000673622	0.04747299	0.485133	1.399715195
NM_020458	TTC7A	0.000676521	0.047602801	0.469612	1.384736707
NM_003784	SERPINB7	0.000678755	0.047638651	1.710382	3.272475387
BC009476	PELI2	0.000679154	0.047638651	-0.74678	-1.678044859
NM_015481	ZNF385	0.000680205	0.047638651	0.919989	1.8921004
NM_003352	SUMO1	0.000685021	0.047764526	0.250882	1.189934372
NM_004047	ATP6V0B	0.000686532	0.047764526	0.487556	1.402067689
BC019348	MGC70863	0.000686616	0.047764526	0.765266	1.699683847

Continued

NM_014223	NFYC	0.000686871	0.047764526	0.605575	1.521584716
BC108908	POLD3	0.000687496	0.047764526	-0.69343	-1.617127755
XM_926355	LOC642535	0.000688366	0.047764526	0.406239	1.325226165
NM_001946	DUSP6	0.00069063	0.047847943	0.493391	1.40775024
NM_001039670	HOM-TES-103	0.000693255	0.047888196	0.474899	1.389820722
BC100018	COMT	0.000693338	0.047888196	0.589414	1.504635737
BC095471	HRAS	0.000696156	0.047993912	1.113787	2.164130184
BC034991	MNS1	0.00069736	0.047993912	-1.18016	-2.266024111
NM_021078	GCN5L2	0.000699006	0.047993912	0.622971	1.540042935
XM_929378	LOC646450	0.000699132	0.047993912	1.152244	2.22259258
XM_209704	LOC653314	0.000701491	0.048082588	0.237471	1.178924333
XM_376342	LOC644162	0.000704249	0.048164703	-0.5508	-1.464895509
BC010991	RBED1	0.000705285	0.048164703	0.631695	1.549383836
NM_199337	LOC374395	0.000705898	0.048164703	0.661341	1.58155216
NM_003086	SNAPC4	0.00070746	0.048190421	0.643353	1.561955105
NM_058191	C21orf66	0.000708415	0.048190421	-0.37267	-1.294743262
BC032947	MTMR1	0.00071187	0.048352415	0.130105	1.09437307
BC044792	AMT	0.000713431	0.048385478	0.52721	1.441139863
AY302071	APTX	0.000715257	0.048431746	0.430191	1.347412412
BC048281	ZRANB1	0.000716389	0.048431746	-0.41267	-1.331148111
NM_016090	RBM7	0.00071734	0.048431746	-0.51903	-1.432994148
NM_014145	C20orf30	0.000721735	0.048655524	0.29365	1.225737801
NM_018683	ZNF313	0.000723195	0.048681066	0.29233	1.224616767
NM_012267	HSPBP1	0.000726383	0.048822679	0.677616	1.599494403
XM_932116	LOC440341	0.000729311	0.048946475	-0.37501	-1.29684773
NM_016581	ECSIT	0.000734144	0.049112906	0.584599	1.499621691
NM_006612	KIF1C	0.000734279	0.049112906	0.829564	1.777148049
NM_016399	TRIAP1	0.00073561	0.049112906	0.891867	1.855576105
AK094016	RFNG	0.000736154	0.049112906	0.753417	1.685780491
BC107682	NDUFC1	0.00074159	0.049402399	0.818284	1.763306806
NM_012151	F8A1	0.000747049	0.049620452	0.322783	1.2507408
NM_004593	SFRS10	0.000747067	0.049620452	-0.45939	-1.374957093
NM_005469	ACOT8	0.000750134	0.049750758	0.522806	1.436746531
NM_031477	YPEL3	0.000754176	0.049945282	0.337014	1.263139089

Supplemental list 2. Annotation of differentially expressed genes in cancer-associated fibroblasts.

GS	SIZE	SOURCE	ES	NES	Tag %	Gene %	Signal	FDR (median)	glob. p.val
RESPONSE_TO_ENDOGENOUS_STIMULUS	85	Genes annotated by the GO term GO:0009719. A change in state or activity of a cell or an organism (in terms of movement, secretion, enzyme production, gene expression, etc.) as a result of an endogenous stimulus.	0.3	1.31	0.27	0.18	0.22	0.32	0.01
MICROTUBULE_BASED_PROCESS	28	Genes annotated by the GO term GO:0007017. Any cellular process that depends upon or alters the microtubule cytoskeleton, that part of the cytoskeleton comprising microtubules and their associated proteins.	0.57	1.31	0.36	0.13	0.31	0.32	0.01
ESTABLISHMENT_AND_OR_MAINTENANCE_OF_CHROMATIN_ARCHITECTURE	27	Genes annotated by the GO term GO:0006325. The specification, formation and maintenance of the physical structure of eukaryotic chromatin.	0.34	1.35	0.41	0.24	0.31	0.28	0.01
PROTEIN_CATABOLIC_PROCESS	20	Genes annotated by the GO term GO:0030163. The chemical reactions and pathways resulting in the breakdown of a protein by the destruction of the native, active configuration, with or without the hydrolysis of peptide bonds.	0.42	1.35	0.1	0.01	0.1	0.28	0.01
CELL_PROLIFERATION_GO_0008283	178	Genes annotated by the GO term GO:0008283. The multiplication or reproduction of cells, resulting in the expansion of a cell population.	0.37	1.33	0.17	0.11	0.15	0.32	0.01
ESTABLISHMENT_OF_CELLULAR_LOCALIZATION	111	Genes annotated by the GO term GO:0051649. The directed movement of a substance or cellular entity, such as a protein complex or organelle, to a specific location within, or in the membrane of, a cell.	0.28	1.34	0.06	0.03	0.06	0.3	0.02
MICROTUBULE_CYTOSKELETON_ORGANIZATION_AND_BIOGENESIS	16	Genes annotated by the GO term GO:0000226. A process that is carried out at the cellular level which results in the formation, arrangement of constituent parts, or disassembly of cytoskeletal structures comprising microtubules and their associated proteins.	0.71	1.36	0.31	0.02	0.31	0.26	0.03
NEGATIVE_REGULATION_OF_PROGRAMMED_CELL_DEATH	50	Genes annotated by the GO term GO:0043069. Any process that stops, prevents or reduces the frequency, rate or extent of programmed cell death, cell death resulting from activation of endogenous cellular processes.	0.24	1.04	0.04	0	0.04	0.7	0.03
REGULATION_OF_DNA_METABOLIC_PROCESS	20	Genes annotated by the GO term GO:0051052. Any process that modulates the frequency, rate or extent of the chemical reactions and pathways involving DNA.	0.54	1.42	0.35	0.16	0.3	0.17	0.04
DNA_METABOLIC_PROCESS	108	Genes annotated by the GO term GO:0006259. The chemical reactions and pathways involving DNA, deoxyribonucleic acid, one of the two main types of nucleic acid, consisting of a long, unbranched macromolecule formed from one, or more commonly, two, strands of linked deoxyribonucleotides.	0.37	1.41	0.31	0.17	0.26	0.16	0.04
RESPONSE_TO_DNA_DAMAGE_STIMULUS	74	Genes annotated by the GO term GO:0006974. A change in state or activity of a cell or an organism (in terms of movement, secretion, enzyme production, gene expression, etc.) as a result of a stimulus indicating damage to its DNA from environmental insults or errors during metabolism.	0.31	1.28	0.28	0.18	0.24	0.43	0.04
INTERPHASE_OF_MITOTIC_CELL_CYCLE	30	Genes annotated by the GO term GO:0051329. Progression through interphase, the stage of cell cycle between successive rounds of mitosis. Canonically, interphase is the stage of the cell cycle during which the biochemical and physiologic functions of the cell are performed and replication of chromatin occurs.	0.65	1.39	0.47	0.16	0.39	0.19	0.05

Continued

DNA_REPAIR	60	Genes annotated by the GO term GO:0006281. The process of restoring DNA after damage. Genomes are subject to damage by chemical and physical agents in the environment (e.g. UV and ionizing radiations, chemical mutagens, fungal and bacterial toxins, etc.) and by free radicals or alkylating agents endogenously generated in metabolism. DNA is also damaged because of errors during its replication. A variety of different DNA repair pathways have been reported that include direct reversal, base excision repair, nucleotide excision repair, photoreactivation, bypass, double-strand break repair pathway, and mismatch repair pathway.	0.33	1.28	0.3	0.18	0.25	0.4	0.05
INTERPHASE	31	Genes annotated by the GO term GO:0051325. Progression through interphase, the stage of cell cycle between s of chromosome segregation. Canonically, interphase is the stage of the cell cycle during which the biochemical and physiologic functions of the cell are performed and replication of chromatin occurs.	0.66	1.42	0.48	0.16	0.41	0.19	0.05
WOUND_HEALING	17	Genes annotated by the GO term GO:0042060. The series of events that restore integrity to a damaged tissue, following an injury.	0.54	1.06	0.35	0.1	0.32	0.7	0.06
CELLULAR_PROTEIN_CATABOLIC_PROCESS	16	Genes annotated by the GO term GO:0044257. The chemical reactions and pathways resulting in the breakdown of a protein by individual cells.	0.49	1.36	0.13	0.01	0.12	0.28	0.06
MITOSIS	40	Genes annotated by the GO term GO:0007067. Progression through mitosis, the division of the eukaryotic cell nucleus to produce two daughter nuclei that, usually, contain the identical chromosome complement to their mother.	0.73	1.42	0.53	0.09	0.48	0.2	0.07
NEGATIVE_REGULATION_OF_CELL_CYCLE	37	Genes annotated by the GO term GO:0045786. Any process that stops, prevents or reduces the rate or extent of progression through the cell cycle.	0.27	1.02	0.16	0.14	0.14	0.78	0.07
NEGATIVE_REGULATION_OF_APOPTOSIS	49	Genes annotated by the GO term GO:0043066. Any process that stops, prevents or reduces the frequency,rate or extent of cell death by apoptosis.	0.24	1.05	0.04	0	0.04	0.73	0.07
RESPONSE_TO_VIRUS	16	Genes annotated by the GO term GO:0009615. A change in state or activity of a cell or an organism (in terms of movement, secretion, enzyme production, gene expression, etc.) as a result of a stimulus from a virus.	0.44	1.06	0.63	0.34	0.41	0.71	0.07
MACROMOLECULE_CATABOLIC_PROCESS	38	Genes annotated by the GO term GO:0009057. The chemical reactions and pathways resulting in the breakdown of a macromolecule, any large molecule including proteins, nucleic acids and carbohydrates.	0.28	1.06	0.08	0.04	0.08	0.72	0.08
REGULATION_OF_MITOSIS	20	Genes annotated by the GO term GO:0007088. Any process that modulates the frequency, rate or extent of mitosis.	0.73	1.42	0.4	0.04	0.39	0.22	0.08
ORGANELLE_ORGANIZATION_AND_BIOGENESIS	171	Genes annotated by the GO term GO:0006996. A process that is carried out at the cellular level which results in the formation, arrangement of constituent parts, or disassembly of any organelle within a cell.	0.31	1.26	0.11	0.06	0.1	0.44	0.09
CELLULAR_MACROMOLECULE_CATABOLIC_PROCESS	25	Genes annotated by the GO term GO:0044265. The chemical reactions and pathways resulting in the breakdown of a macromolecule, any large molecule including proteins, nucleic acids and carbohydrates, as carried out by individual cells.	0.36	1.25	0.08	0.01	0.08	0.46	0.09
M_PHASE	54	Genes annotated by the GO term GO:0000279. Progression through M phase, the part of the cell cycle comprising nuclear division.	0.7	1.43	0.46	0.09	0.42	0.23	0.11
ANTI_APOPTOSIS	40	Genes annotated by the GO term GO:0006916. A process which directly inhibits any of the steps required for cell death by apoptosis.	0.27	1.07	0.05	0	0.05	0.74	0.11

Continued

BIOPOLYMER_ CATABOLIC_ PROCESS	37	Genes annotated by the GO term GO:0043285. The chemical reactions and pathways resulting in the breakdown of biopolymers, long, repeating chains of monomers found in nature e.g. polysaccharides and proteins.	0.29	1.06	0.08	0.04	0.08	0.73	0.11
REGULATION_OF_ PHOSPHORYLATION	16	Genes annotated by the GO term GO:0042325. Any process that modulates the frequency, rate or extent of addition of phosphate groups into a molecule.	0.39	1.18	0.25	0.12	0.22	0.63	0.12
M_PHASE_OF_MITOTIC_ CELL_CYCLE	42	Genes annotated by the GO term GO:0000087. Progression through M phase, the part of the mitotic cell cycle during which mitosis takes place.	0.74	1.43	0.52	0.09	0.48	0.22	0.12
NEGA- TIVE_REGULATION_ OF_NUCLEOBASE_ NUCLEOSIDE_ NUCLEOTIDE_AND_ NUCLEIC_ACID_ METABOLIC_PROCESS	78	Genes annotated by the GO term GO:0045934. Any process that stops, prevents or reduces the frequency, rate or extent of the chemical reactions and pathways involving nucleobases, nucleosides, nucleotides and nucleic acids.	0.24	1.07	0.09	0.04	0.09	0.75	0.13
DNA_RECOMBINATION	23	Genes annotated by the GO term GO:0006310. The processes by which a new genotype is formed by reassortment of genes resulting in gene combinations different from those that were present in the parents. In eukaryotes genetic recombination can occur by chromosome assortment, intrachromosomal recombination, or nonreciprocal interchromosomal recombination. Intrachromosomal recombination occurs by crossing over. In bacteria it may occur by genetic transformation, conjugation, transduction, or F-duction.	0.46	1.48	0.39	0.17	0.33	0.15	0.13
CHROMATIN_ MODIFICATION	19	Genes annotated by the GO term GO:0016568. The alteration of DNA or protein in chromatin, which may result in changing the chromatin structure.	0.27	1.02	0.37	0.23	0.28	0.8	0.13
DNA_REPLICATION	43	Genes annotated by the GO term GO:0006260. The process whereby new strands of DNA are synthesized. The template for replication can either be an existing DNA molecule or RNA.	0.58	1.51	0.51	0.2	0.41	0.18	0.14
HEMOSTASIS	17	Genes annotated by the GO term GO:0007599. The stopping of bleeding (loss of body fluid) or the arrest of the circulation to an organ or part.	0.57	1.16	0.35	0.1	0.32	0.66	0.14
NEGA- TIVE_REGULATION_ OF_CELLULAR_ METABOLIC_PROCESS	95	Genes annotated by the GO term GO:0031324. Any process that stops, prevents or reduces the frequency, rate or extent of the chemical reactions and pathways by which individual cells transform chemical substances.	0.23	1.09	0.12	0.1	0.11	0.75	0.14
NEGATIVE_ REGULATION_OF_ METABOLIC_PROCESS	95	Genes annotated by the GO term GO:0009892. Any process that stops, prevents or reduces the frequency, rate or extent of the chemical reactions and pathways within a cell or an organism.	0.23	1.09	0.12	0.1	0.11	0.75	0.14
UBIQUITIN_CYCLE	15	Genes annotated by the GO term GO:0006512. The cyclical process by which one or more ubiquitin moieties are added to (ubiquitination) and removed from (deubiquitination) a protein.	0.38	1.19	0.27	0.12	0.24	0.65	0.15
CHROMOSOME_ ORGANIZATION_ AND_BIOGENESIS	43	Genes annotated by the GO term GO:0051276. A process that is carried out at the cellular level that results in the formation, arrangement of constituent parts, or disassembly of chromosomes, structures composed of a very long molecule of DNA and associated proteins that carries hereditary information.	0.52	1.46	0.44	0.24	0.34	0.21	0.15
CELL_CYCLE_ CHECKPOINT_ GO_0000075	25	Genes annotated by the GO term GO:0000075. A point in the eukaryotic cell cycle where progress through the cycle can be halted until conditions are suitable for the cell to proceed to the next stage.	0.66	1.43	0.52	0.16	0.44	0.24	0.15

Continued

REPRODUCTIVE_ PROCESS	39	Genes annotated by the GO term GO:0022414. A biological process that directly contributes to the process of producing new individuals by one or two organisms. The new individuals inherit some proportion of their genetic material from the parent or parents.	0.33	1.17	0.21	0.17	0.17	0.64	0.15
REGULATION_ OF_PROTEIN_ MODIFICATION_ PROCESS	15	Genes annotated by the GO term GO:0031399. Any process that modulates the frequency, rate or extent of the covalent alteration of one or more amino acid residues within a protein.	0.36	1.15	0.2	0.12	0.18	0.7	0.16
DNA_DEPENDENT_ DNA_REPLICATION	25	Genes annotated by the GO term GO:0006261. The process whereby new strands of DNA are synthesized, using parental DNA as a template for the DNA-dependent DNA polymerases that synthesize the new strands.	0.62	1.49	0.48	0.17	0.4	0.17	0.16
NEGATIVE_ REGULATION_OF_ DEVELOPMENTAL_ PROCESS	63	Genes annotated by the GO term GO:0051093. Any process that stops, prevents or reduces the rate or extent of development, the biological process whose specific outcome is the progression of an organism over time from an initial condition (e.g. a zygote, or a young adult) to a later condition (e.g. a multicellular animal or an aged adult).	0.23	1.08	0.16	0.16	0.13	0.78	0.16
RESPONSE_TO_STRESS	182	Genes annotated by the GO term GO:0006950. A change in state or activity of a cell or an organism (in terms of movement, secretion, enzyme production, gene expression, etc.) as a result of a stimulus indicating the organism is under stress. The stress is usually, but not necessarily, exogenous (e.g. temperature, humidity, ionizing radiation).	0.22	1.07	0.22	0.21	0.18	0.77	0.16
CELL_CYCLE_ARREST_ GO_0007050	25	Genes annotated by the GO term GO:0007050. Any process by which progression through the cell cycle is halted during one of the normal phases (G1, S, G2, M).	0.28	0.99	0.16	0.14	0.14	0.81	0.17
NEGA- TIVE_REGULATION_ OF_CATALYTIC_ACTIVIT Y	22	Genes annotated by the GO term GO:0043086. Any process that stops or reduces the activity of an enzyme.	0.4	1.19	0.18	0.11	0.16	0.65	0.17
CYTOSKELETON_ ORGANIZATION_ AND_BIOGENESIS	70	Genes annotated by the GO term GO:0007010. A process that is carried out at the cellular level which results in the formation, arrangement of constituent parts, or disassembly of cytoskeletal structures.	0.41	1.19	0.37	0.24	0.28	0.65	0.17
MONOCARBOX- YLIC_ACID_ METABOLIC_PROCESS	32	Genes annotated by the GO term GO:0032787. The chemical reactions and pathways involving monocarboxylic acids, any organic acid containing one carboxyl (COOH) group or anion (COO-).	0.25	0.97	0.31	0.23	0.24	0.83	0.18
FEMALE_PREGNANCY	15	Genes annotated by the GO term GO:0007565. The physiological processes that allow an embryo or foetus to develop within the body of a female animal. It covers the time from fertilization of a female ovum by a male spermatozoon until birth.	0.3	0.99	0.27	0.17	0.22	0.82	0.18
REGULATION_OF_ CELL_CYCLE	89	Genes annotated by the GO term GO:0051726. Any process that modulates the rate or extent of progression through the cell cycle.	0.47	1.51	0.33	0.17	0.27	0.17	0.19
NEGA- TIVE_REGULATION_ OF_BIOLOGICAL_PROCES S	226	Genes annotated by the GO term GO:0048519. Any process that stops, prevents or reduces the frequency, rate or extent of a biological process. Biological processes are regulated by many means; examples include the control of gene expression, protein modification or interaction with a protein or substrate molecule.	0.22	1.13	0.17	0.17	0.15	0.76	0.19
REGULATION_OF_ CYCLIN_DEPENDENT_ PROTEIN_KINASE_ ACTIVITY	25	Genes annotated by the GO term GO:0000079. Any process that modulates the frequency, rate or extent of CDK activity.	0.32	0.99	0.16	0.07	0.15	0.83	0.2

Continued

STRIATED_MUSCLE_DEVELOPMENT	20	Genes annotated by the GO term GO:0014706. The process whose specific outcome is the progression of a striated muscle over time, from its formation to the mature structure. Striated muscle contain fibers that are divided by transverse bands into striations, and cardiac and skeletal muscle are types of striated muscle. Skeletal muscle myoblasts fuse to form myotubes and eventually multinucleated muscle fibers. The fusion of cardiac cells is very rare and can only form binucleate cells.	0.35	0.97	0.2	0.15	0.17	0.84	0.22
GAMETE_GENERATION	30	Genes annotated by the GO term GO:0007276. The generation and maintenance of gametes. A gamete is a haploid reproductive cell.	0.36	1.09	0.43	0.29	0.31	0.78	0.23
LOCOMOTORY_BEHAVIOR	28	Genes annotated by the GO term GO:0007626. The specific movement from place to place of an organism in response to external or internal stimuli. Locomotion of a whole organism in a manner dependent upon some combination of that organism's internal state and external conditions.	0.25	0.59	0.43	0.3	0.3	0.99	0.24
PROTEIN_MODIFICATION_BY_SMALL_PROTEIN_CONJUGATION	15	Genes annotated by the GO term GO:0032446. A process by which one or more moieties of a small protein, such as ubiquitin or a ubiquitin-like protein, are covalently attached to a target protein.	0.35	1.11	0.13	0.03	0.13	0.76	0.24
CELL_CYCLE_PHASE	78	Genes annotated by the GO term GO:0022403. A cell cycle process comprising the steps by which a cell progresses through one of the biochemical and morphological phases and events that occur during successive cell replication or nuclear replication events.	0.67	1.52	0.54	0.16	0.46	0.22	0.25
FATTY_ACID_METABOLIC_PROCESS	20	Genes annotated by the GO term GO:0006631. The chemical reactions and pathways involving fatty acids, aliphatic monocarboxylic acids liberated from naturally occurring fats and oils by hydrolysis.	0.33	1.11	0.3	0.23	0.23	0.77	0.25
CELL_CYCLE_PROCESS	91	Genes annotated by the GO term GO:0022402. A cellular process that is involved in the progression of biochemical and morphological phases and events that occur in a cell during successive cell replication or nuclear replication events.	0.68	1.55	0.54	0.16	0.46	0.18	0.25
NEGATIVE_REGULATION_OF_CELLULAR_PROCESS	219	Genes annotated by the GO term GO:0048523. Any process that stops, prevents or reduces the frequency, rate or extent of cellular processes, those that are carried out at the cellular level, but are not necessarily restricted to a single cell. For example, cell communication occurs among more than one cell, but occurs at the cellular level.	0.21	1.09	0.16	0.17	0.14	0.79	0.26
RESPONSE_TO_CHEMICAL_STIMULUS	108	Genes annotated by the GO term GO:0042221. A change in state or activity of a cell or an organism (in terms of movement, secretion, enzyme production, gene expression, etc.) as a result of a chemical stimulus.	0.14	0.51	0.22	0.23	0.17	0.99	0.27
REGULATION_OF_BODY_FLUID_LEVELS	19	Genes annotated by the GO term GO:0050878. Any process that modulates the levels of body fluids.	0.5	1.1	0.32	0.1	0.28	0.77	0.27
DEFENSE_RESPONSE	63	Genes annotated by the GO term GO:0006952. Reactions, triggered in response to the presence of a foreign body or the occurrence of an injury, which result in restriction of damage to the organism attacked or prevention/recovery from the infection caused by the attack.	0.18	0.54	0.19	0.19	0.16	0.99	0.27

Continued

REGULATION_OF_RESPONSE_TO_STIMULUS	22	Genes annotated by the GO term GO:0048583. Any process that modulates the frequency, rate or extent of a response to a stimulus. Response to stimulus is a change in state or activity of a cell or an organism (in terms of movement, secretion, enzyme production, gene expression, etc.) as a result of a stimulus.	0.22	0.61	0.18	0.17	0.15	0.98	0.3
MITOTIC_CELL_CYCLE	80	Genes annotated by the GO term GO:0000278. Progression through the phases of the mitotic cell cycle, the most common eukaryotic cell cycle, which canonically comprises four successive phases called G1, S, G2, and M and includes replication of the genome and the subsequent segregation of chromosomes into daughter cells. In some variant cell cycles nuclear replication or nuclear division may not be followed by cell division, or G1 and G2 phases may be absent.	0.67	1.56	0.44	0.12	0.39	0	0.3
CELL_CYCLE_GO_0007049	152	Genes annotated by the GO term GO:0007049. The progression of biochemical and morphological phases and events that occur in a cell during successive cell replication or nuclear replication events. Canonically, the cell cycle comprises the replication and segregation of genetic material followed by the division of the cell, but in endocycles or syncytial cells nuclear replication or nuclear division may not be followed by cell division.	0.57	1.58	0.4	0.17	0.34	0	0.32
RESPONSE_TO_OXIDATIVE_STRESS	22	Genes annotated by the GO term GO:0006979. A change in state or activity of a cell or an organism (in terms of movement, secretion, enzyme production, gene expression, etc.) as a result of oxidative stress, a state often resulting from exposure to high levels of reactive oxygen species, e.g. superoxide anions, hydrogen peroxide (H2O2), and hydroxyl radicals.	0.18	0.62	0.41	0.31	0.28	0.99	0.39
NUCLEO-BASE_NUCLEOSIDE_NUCLEOTIDE_AND_NUCLEIC_ACID_METABOLIC_PROCESS	407	Genes annotated by the GO term GO:0006139. The chemical reactions and pathways involving nucleobases, nucleosides, nucleotides and nucleic acids.	0.16	0.92	0.19	0.22	0.16	0.96	0.4
GENERATION_OF_NEURONS	28	Genes annotated by the GO term GO:0048699. The process by which nerve cells are generated. This includes the production of neuroblasts and their differentiation into neurons.	0.3	0.92	0.29	0.19	0.23	0.96	0.4
REGULATION_OF_CATALYTIC_ACTIVITY	91	Genes annotated by the GO term GO:0050790. Any process that modulates the activity of an enzyme.	0.21	0.9	0.13	0.11	0.12	0.95	0.4
NEUROGENESIS	29	Genes annotated by the GO term GO:0022008. Generation of cells within the nervous system.	0.29	0.9	0.28	0.19	0.22	0.96	0.41
REGULATION_OF_TRANSCRIPTION_FROM_RNA_POLYMERASE_II_PROMOTER	88	Genes annotated by the GO term GO:0006357. Any process that modulates the frequency, rate or extent of transcription from an RNA polymerase II promoter.	0.2	0.89	0.06	0.03	0.06	0.98	0.42
REGULATION_OF_MULTICELLULAR_ORGANISMAL_PROCESS	49	Genes annotated by the GO term GO:0051239. Any process that modulates the frequency, rate or extent of an organismal process, the processes pertinent to the function of an organism above the cellular level; includes the integrated processes of tissues and organs.	0.24	0.9	0.2	0.17	0.17	0.97	0.45
GROWTH	26	Genes annotated by the GO term GO:0040007. The increase in size or mass of an entire organism, a part of an organism or a cell.	0.21	0.64	0.12	0.07	0.11	1	0.52

Continued

CELL_DEVELOPMENT	188	Genes annotated by the GO term GO:0048468. The process whose specific outcome is the progression of the cell over time, from its formation to the mature structure. Cell development does not include the steps involved in committing a cell to a specific fate.	0.19	0.87	0.09	0.08	0.08	1	0.54
NEGA-TIVE_REGULATION_OF_TRANSCRIPTION_FROM_RNA_POLYMERASE_II_PROMOTER	31	Genes annotated by the GO term GO:0000122. Any process that stops, prevents or reduces the frequency, rate or extent of transcription from an RNA polymerase II promoter.	0.17	0.67	0.16	0.16	0.14	1	0.54
ACTIN_FILAMENT_BASED_PROCESS	40	Genes annotated by the GO term GO:0030029. Any cellular process that depends upon or alters the actin cytoskeleton, that part of the cytoskeleton comprising actin filaments and their associated proteins.	0.23	0.83	0.38	0.26	0.28	1	0.54
STRESS_ACTIVATED_PROTEIN_KINASE_SIGNALING_PATHWAY	18	Genes annotated by the GO term GO:0031098. A series of molecular signals in which a stress-activated protein kinase (SAPK) cascade relays one or more of the signals.	0.16	0.62	0.06	0.03	0.05	1	0.57
POSITIVE_REGULATION_OF_CELLULAR_PROCESS	224	Genes annotated by the GO term GO:0048522. Any process that activates or increases the frequency, rate or extent of cellular processes, those that are carried out at the cellular level, but are not necessarily restricted to a single cell. For example, cell communication occurs among more than one cell, but occurs at the cellular level.	0.16	0.68	0.07	0.08	0.07	1	0.58
POSITIVE_REGULATION_OF_BIOLOGICAL_PROCESSES	234	Genes annotated by the GO term GO:0048518. Any process that activates or increases the frequency, rate or extent of a biological process. Biological processes are regulated by many means; examples include the control of gene expression, protein modification or interaction with a protein or substrate molecule.	0.16	0.65	0.07	0.08	0.06	1	0.58
REGULATION_OF_CELLULAR_COMPONENT_ORGANIZATION_AND_BIOGENESIS	37	Genes annotated by the GO term GO:0051128. Any process that modulates the frequency, rate or extent of the processes involved in the formation, arrangement of constituent parts, or disassembly of cell structures, including the plasma membrane and any external encapsulating structures such as the cell wall and cell envelope.	0.16	0.68	0.41	0.33	0.27	1	0.59
ACTIN_CYTOSKELETON_ORGANIZATION_AND_BIOGENESIS	37	Genes annotated by the GO term GO:0030036. A process that is carried out at the cellular level which results in the formation, arrangement of constituent parts, or disassembly of cytoskeletal structures comprising actin filaments and their associated proteins.	0.25	0.84	0.41	0.26	0.3	1	0.59
CELLULAR_PROTEIN_COMPLEX_ASSEMBLY	15	Genes annotated by the GO term GO:0043623. The aggregation, arrangement and bonding together of a set of components to form a protein complex, occurring at the level of an individual cell.	0.29	0.83	0.13	0.08	0.12	1	0.59
REGULATION_OF_NUCLEOBASE_NUCLEOSIDE_NUCLEOTIDE_AND_NUCLEIC_ACID_METABOLIC_PROCESS	206	Genes annotated by the GO term GO:0019219. Any process that modulates the frequency, rate or extent of the chemical reactions and pathways involving nucleobases, nucleosides, nucleotides and nucleic acids.	0.16	0.84	0.05	0.04	0.05	1	0.59

Continued

MUSCLE_DEVELOPMENT	42	Genes annotated by the GO term GO:0007517. The process whose specific outcome is the progression of the muscle over time, from its formation to the mature structure. The muscle is an organ consisting of a tissue made up of various elongated cells that are specialized to contract and thus to produce movement and mechanical work.	0.22	0.85	0.12	0.15	0.1	1	0.6
REGULATION_OF_DEVELOPMENTAL_PROCESS	150	Genes annotated by the GO term GO:0050793. Any process that modulates the frequency, rate or extent of development, the biological process whose specific outcome is the progression of a multicellular organism over time from an initial condition (e.g. a zygote, or a young adult) to a later condition (e.g. a multicellular animal or an aged adult).	0.19	0.82	0.07	0.08	0.07	1	0.61
NEGATIVE_REGULATION_OF_CELL_PROLIFERATION	54	Genes annotated by the GO term GO:0008285. Any process that stops, prevents or reduces the rate or extent of cell proliferation.	0.28	0.84	0.07	0.02	0.07	1	0.61
REGULATION_OF_HYDROLASE_ACTIVITY	23	Genes annotated by the GO term GO:0051336. Any process that modulates the frequency, rate or extent of hydrolase activity, the catalysis of the hydrolysis of various bonds, e.g. C-O, C-N, C-C, phosphoric anhydride bonds, etc. Hydrolase is the systematic name for any enzyme of EC class 3.	0.26	0.81	0.04	0	0.04	1	0.62
APOPTOTIC_PROGRAM	19	Genes annotated by the GO term GO:0008632. The intracellular signaling cascade that results when a cell is triggered to undergo apoptosis.	0.24	0.79	0.11	0.08	0.1	1	0.64
TISSUE_DEVELOPMENT	41	Genes annotated by the GO term GO:0009888. The process whose specific outcome is the progression of a tissue over time, from its formation to the mature structure.	0.22	0.77	0.29	0.24	0.23	1	0.64
TRANSCRIPTION_FROM_RNA_POLYMERASE_II_PROMOTER	135	Genes annotated by the GO term GO:0006366. The synthesis of RNA from a DNA template by RNA polymerase II (Pol II), originating at a Pol II-specific promoter. Includes transcription of messenger RNA (mRNA) and certain small nuclear RNAs (snRNAs).	0.15	0.68	0.04	0.03	0.04	1	0.65
BEHAVIOR	42	Genes annotated by the GO term GO:0007610. The specific actions or reactions of an organism in response to external or internal stimuli. Patterned activity of a whole organism in a manner dependent upon some combination of that organism's internal state and external conditions.	0.26	0.7	0.31	0.24	0.24	1	0.67
SKELETAL_DEVELOPMENT	39	Genes annotated by the GO term GO:0001501. The process whose specific outcome is the progression of the skeleton over time, from its formation to the mature structure. The skeleton is the bony framework of the body in vertebrates (endoskeleton) or the hard outer envelope of insects (exoskeleton or dermoskeleton).	0.22	0.78	0.15	0.15	0.13	1	0.67
RESPONSE_TO_OTHER_ORGANISM	19	Genes annotated by the GO term GO:0051707. A change in state or activity of a cell or an organism (in terms of movement, secretion, enzyme production, gene expression, etc.) as a result of a stimulus from another living organism.	0.27	0.71	0.32	0.24	0.24	1	0.68
SENSORY_PERCEPTION	45	Genes annotated by the GO term GO:0007600. The series of events required for an organism to receive a sensory stimulus, convert it to a molecular signal, and recognize and characterize the signal.	0.19	0.73	0.16	0.14	0.14	1	0.69
NEGATIVE_REGULATION_OF_PROTEIN_METABOLIC_PROCESS	16	Genes annotated by the GO term GO:0051248. Any process that stops, prevents or reduces the frequency, rate or extent of chemical reactions and pathways involving a protein.	0.19	0.7	0.13	0.17	0.11	1	0.69

Continued

NEGA-TIVE_REGULATION_OF_CELLULAR_PROTEIN	15	Genes annotated by the GO term GO:0032269. Any process that stops, prevents or reduces the frequency, rate or extent of the chemical reactions and pathways involving a protein, occurring at the level of an individual cell.	0.2	0.72	0.13	0.17	0.11	1	0.7
METABOLIC_PROCESS		Genes annotated by the GO term GO:0009790. The process whose specific outcome is the progression of an embryo from its formation until the end of its embryonic life stage. The end of the embryonic stage is organism-specific. For example, for mammals, the process would begin with zygote formation and end with birth. For insects, the process would begin at zygote formation and end with larval hatching. For plant zygotic embryos, this would be from zygote formation to the end of seed dormancy. For plant vegetative embryos, this would be from the initial determination of the cell or group of cells to form an embryo until the point when the embryo becomes independent of the parent plant.							
EMBRYONIC_DEVELOPMENT	26	Genes annotated by the GO term GO:0007519. The developmental sequence of events leading to the formation of adult muscle that occurs in the anima. In vertebrate skeletal muscle the main events are: the fusion of myoblasts to form myotubes that increase in size by further fusion to them of myoblasts, the formation of myofibrils within their cytoplasm and the establishment of functional neuromuscular junctions with motor neurons. At this stage they can be regarded as mature muscle fibers.	0.25	0.73	0.15	0.11	0.14	1	0.72
SKELETAL_MUSCLE_DEVELOPMENT	15	Genes annotated by the GO term GO:0051704. The processes by which an organism has an effect on another organism of the same or different species.	0.26	0.73	0.2	0.15	0.17	1	0.75
MULTI_ORGANISM_PROCESS	42	Genes annotated by the GO term GO:0042127. Any process that modulates the frequency, rate or extent of cell proliferation.	0.23	0.73	0.29	0.25	0.22	1	0.75
REGULATION_OF_CELL_PROLIFERATION	106		0.21	0.73	0.16	0.16	0.14	1	0.76